Differential Roles of Hsp70 and Hsp90 in the Assembly of the Replicase Complex of a Positive-Strand RNA Plant Virus

Akira Mine,[a*] Kiwamu Hyodo,[a] Yuri Tajima,[a] Kusumawaty Kusumanegara,[a] Takako Taniguchi,[b] Masanori Kaido,[a] Kazuyuki Mise,[a] Hisaaki Taniguchi,[b] and Tetsuro Okuno[a]

Laboratory of Plant Pathology, Graduate School of Agriculture, Kyoto University, Sakyo-ku, Kyoto 606-8502, Japan[a]; Institute for Enzyme Research, University of Tokushima, Tokushima 770-8503, Japan[b]

Address correspondence to Tetsuro Okuno, okuno@kais.kyoto-u.ac.jp.

*Present address: Department of Plant Microbe Interactions Max Planck Institute for Plant Breeding Research, Carl-von-Linne Weg 10, 50829 Cologne, Germany.

Running Title: Chaperone-Assisted Assembly of Viral Replicase

.

Abstract

Assembly of viral replicase complexes of eukaryotic positive-strand RNA viruses is a regulated process: multiple viral and host components must be assembled on intracellular membranes and ordered into quaternary complexes capable of synthesizing viral RNAs. However, the molecular mechanisms underlying this process are poorly understood. In this study, we used a model virus, *Red clover necrotic mosaic virus* (RCNMV), whose replicase complex can be detected readily as the 480-kDa functional protein complex. We found that host heat shock proteins Hsp70 and Hsp90 are required for RCNMV RNA replication and that they interact with p27, a viral-encoded component of the 480-kDa replicase complex, on the endoplasmic reticulum membrane. Using a cell-free viral translation/replication system in combination with specific inhibitors of Hsp70 and Hsp90, we found that inhibition of p27-Hsp70 interaction inhibits the formation of 480-kDa complex but instead induces the accumulation of large complexes that is nonfunctional in viral RNA synthesis. In contrast, inhibition of p27-Hsp90 interaction did not induce such large complexes, but rendered p27 incapable of binding to a specific viral RNA element, which is a critical step for the assembly of the 480-kDa replicase complex and viral RNA replication. Together, our results suggest that Hsp70 and Hsp90 regulate different steps in the assembly of the RCNMV replicase complex.

INTRODUCTION

Most plant and animal viruses are positive-strand RNA viruses, which have single-stranded messenger-sense genomic RNAs. These viruses often induce host membrane rearrangements to form organelle-like compartments in which viral genomic RNAs are replicated via negative-strand RNA intermediates by the viral replicase complexes (10). Viral replicase complexes comprise multiple proteins, including viral auxiliary proteins, viral RNA-dependent RNA polymerase (RdRP), and host proteins (61). Viral replicase complexes have been studied extensively by characterizing their RdRP activities and the functions of the viral and host components of the complexes. These studies have provided important information about the mechanisms regulating genome replication (15, 19, 47, 90), viral pathogenicity (68, 69), and virus–host interactions (24, 25, 32, 33). However, an important question remains: how do multiple viral and host components assemble properly into the replicase complex?

Molecular chaperones are essential for cell viability by ensuring folding of newly synthesized proteins, refolding of misfolded or aggregated proteins, protein complex assembly and disassembly, membrane translocation of organellar and secretory proteins, protein degradation, and activities of regulatory proteins in signal transduction pathways (12, 18, 51). In eukaryotic cells, the abundant and highly conserved molecular chaperones heat shock proteins Hsp70 and Hsp90 play central roles in the biological processes mentioned above, and the activities of Hsp70 and Hsp90 are modulated by a variety of co-chaperones (37, 80). Considering their pivotal roles in cells, it is not surprising that Hsp70 and Hsp90 are involved together with their co-chaperones in virus infection (62). For instance, Hsp70 facilitates the assembly and disassembly of viral capsids (7, 26, 46), promotes the subcellular transport of tombusvirus replicase proteins and affects the activity or assembly of tombusvirus replicase complexes (71, 91),

controls potyvirus gene expression in cooperation with its co-chaperone CPIP (17), and positively and negatively affects the genome replication of various viruses (5, 45, 87, 92). Hsp90 affects the early stages of *Bamboo mosaic virus* (BaMV) infection by binding to the genomic RNA (20), increases the synthesis or stability of viral proteins (4, 8), supports the assembly and nuclear import of influenza A virus RNA polymerase complex (59, 63), and tightly regulates hepatitis C virus replication in cooperation with FKBP8 and hB-ind1 co-chaperones (67, 79, 89).

Hsp70 and Hsp90 sometimes work together in the activation or maturation of viral and cellular proteins. For example, Hsp90 together with Hsp70 and a variety of co-chaperones regulate the actions of steroid receptors and the responses to ligands (16). It has been reported recently that Hsp70, Hsp90, and their co-chaperones facilitate the incorporation of small RNAs into Argonaute proteins, which play central roles in post-transcriptional gene silencing (22, 23, 31, 55). In the case of hepadnavirus reverse transcriptase, Hsp70 and Hsp40 co-chaperone are essential for the specific binding of the reverse transcriptase to pre-genomic RNA templates, and Hsp90 facilitates this step (77, 78). However, the coordinate functions of these molecular chaperones in other biological processes such as multicomponent complex assembly are poorly understood.

To elucidate the molecular mechanisms of the replication of positive-strand RNA viruses, we used *Red clover necrotic mosaic virus* (RCNMV) as a model. RCNMV is a positive-strand RNA plant virus and a member of the genus *Dianthovirus* in the family *Tombusviridae*. The bipartite genomic RNAs, RNA1 and RNA2, possess neither a cap structure at the 5′ end (58) nor a poly(A) tail at the 3′ end (48, 96). Instead, RNA1 and RNA2 use distinct cap/poly(A)-independent mechanisms to produce all viral proteins (30, 57, 58, 74). RNA1 encodes N-terminally overlapping replicase component proteins, a 27-kDa auxiliary protein (p27), and an 88-kDa protein with an RdRP motif (p88). p88 is produced via programmed –1 position ribosomal frameshifting (81, 95). RNA1 also

encodes a coat protein (CP), which is translated from CP subgenomic RNA (76, 86). A small noncoding RNA (SR1f) with a potential function in regulating RCNMV infection is generated from RNA1. RNA2 encodes a movement protein that is required for viral movement in plants (34, 36, 94).

We have developed a model to study the assembly processes of viral replicase complexes by detecting the RCNMV replicase complex as a functional protein complex with an apparent molecular mass of 480 kDa using blue native polyacrylamide gel electrophoresis (BN-PAGE) (53). The 480-kDa replicase complexes are tightly associated with the membrane of the endoplasmic reticulum (ER) and retain the ability to synthesize complementary RNAs by specifically recognizing RCNMV RNAs (41, 53). The assembly of the 480-kDa replicase complex requires both p27–p27 and p27–p88 interactions (52). In addition to p27 and p88, the 480-kDa complexes contain several host proteins, whereas p27 and p88 seem to interact with both the host components of the 480-kDa complex and many other host proteins including chaperones, ribosomal proteins and cytoskeletal proteins, which are absent in the complex (53).

The functions of p27 and p88 in viral RNA replication have been investigated. Both p27 and p88 interact with RNA1 in a translation-coupled manner (27), and these interactions are important for the *cis*-preferential replication of RNA1 (66). p27 but not p88 binds specifically to the Y-shaped RNA element (YRE) of RNA2 in *trans* (27), and this interaction is essential for the recruitment of RNA2 into replication (1, 21). By contrast, the functions of host proteins in RCNMV RNA replication are currently unknown.

In this study, we investigated the functions of two host molecular chaperones, Hsp70 and Hsp90, in RCNMV RNA replication. Gene silencing and pharmacological inhibition of Hsp70 and Hsp90 revealed that these molecular chaperones are required

for RCNMV RNA replication. A series of *in vivo* and *in vitro* protein interaction experiments showed that both Hsp70 and Hsp90 interact with p27 via protein–protein contacts on the ER membrane. Further studies using a cell-free viral translation/replication system showed that when p27-Hsp70 interaction is blocked, p27 form large complexes that are nonfunctional in viral RNA synthesis. In contrast, in the absence of p27-Hsp90 interaction, p27 was unable to bind to a viral RNA element, such as YRE, which is a critical step for the assembly of the 480-kDa replicase complexes. These results provide strong evidence that Hsp70 and Hsp90 have different functions in regulating the assembly of the RCNMV replicase complex.

MATERIALS AND METHODS

Molecular cloning and plasmid construction. pUCR1 (84) and pRC2|G (97) are full-length cDNA clones of RNA1 and RNA2 of RCNMV Australian strain, respectively. pBI_C-CY, pBI_C-NY, pBI_N-NY and pBI_N-CY were kind gifts from Dr. Takashi Araki (Kyoto University, Kyoto, Japan). Constructs described previously that used in this study include pBICp35 (83), pBICp19 (83), pBICB3aGFP (35), pBICRMsG (36), pBICER:mCherry (34), pBICRC1 (84), pUBRC1 (84), pBICRC2 (84), pUBRC2 (84), pUBp35 (80), pUBp88 (81), pBICp27 (84), pBICp88 (84), pBICp27-FLAG (53), pBICp27-HA (51), pUCp27-FLAG (52), pUCp88-T7 (52), pBYL2 (52), pBINTRA6 (73), pTV00 (73), pPVX.NbHsp70c-1 (38) and pBE2113-GUS (54). pET42a and pUC118 were purchased from TAKARA Bio Inc. (Shiga, Japan). *Escherichia coli* DH5α was used for the construction of all plasmids, except that *E. Coli* Top10 (Invitrogen, Carlsbad, CA) was used for the construction of pBYLHsp70. All plasmids constructed in this study were verified by sequencing.

(i) pBYLHsp70 and pBYLHsp90. To isolate Tobacco BY-2 *Hsp70* and *Hsp90* cDNA fragments by reverse transcription-polymerase chain reaction (RT-PCR), we

used two sets of degenerate primers, Hsp70deg-F (5′-AARAAYCARGTNGCNATGAA-3′) plus Hsp70deg-R (5′-CATNCGYTCDATYTCYTCYTT-3′), and Hsp90deg-F (5′-AAGGCGCGCCATGGCGGABRCAGAGACGTTT-3′) plus Hsp90deg-R (5′-AAGGCGCGCCTTAGTCAACYTCCTCCATCTT-3′), respectively. Both 5′-rapid amplification of cDNA ends (5′-RACE) and 3′-RACE techniques were carried out to identify the both ends. Full-length *Hsp70* and *Hsp90* cDNAs were amplified with RT-PCR using the primer pair sets, *Asc*I/Hsp70-F (5′-AACCGGTTGGCGCGCCATGGCAGGAAAAGGTGAAGG-3′) plus *Asc*I/Hsp70-R (5′-AACCGGTTGGCGCGCCAACACCAACAGCTTAGTC-3′), and *Asc*I/Hsp90-F (5′-AAGGCGCGCCATGGCGGACACAGAGACGTTTGC-3′) plus *Asc*I/Hsp90-R (5′-AAGGCGCGCCTTAGTCAACCTCCTCCATCTTGC3′), respectively. The amplified DNAs were digested with *Asc*I and inserted into pBYL2 that had been cut with the same restriction enzyme.

(ii) pTVHsp70. The partial fragment of *NbHsp70c-1* was amplified from pPVX.NbHsp70c-1 (38) using *Sma*I/70-F (5′-GGGGGGCCCGGGTAACGAGAAGGTGCAGG-3′) and *Bam*HI/70-R (5′-CGCGGATCCATTGGCGTCGATGTCAAAG-3′). The amplified DNA was digested with *Sma*I and *Bam*HI, and inserted into pTV00 that had been cut with the same restriction enzymes.

(iii) pBICAscII. An AscI linker (5'-GATCTGGCGCGCC-3') was treated with T4 polynucleotide kinase (New England Biolabs, Ipswich, MA), followed by annealing. The annealed linker was then inserted into pBICp35, which had been digested with BamHI.

(iv) pBICHsp70. The Hsp70 sequence was amplified from pBYLHsp70 using *Bam*HI/Hsp70-F

(5′-ACGGGGATCCAAGGAGATATAACAATGGCAGGAAAAGGTGAAGGA-3′) and *Bam*HI-Hsp70-R (5′-ACGGGGATCCTTAGTCGACCCTCAATC-3′), digested with *Bam*HI and inserted into pBICp35 that had been cut with the same restriction enzyme.

(v) pBICHsp90. pBYLHsp90 was cut with *Asc*I. Then, the resulting 2.1 kilobase fragment was ligated with *Asc*I-digested pBICAscII.

(vi) pBICHA:cYFP and pBICmyc:nYFP. The sequence of HA-tagged cYFP or myc-tagged nYFP was amplified from pBICp27-HA:cYFP using *Stu*I-HA/cYFP-F (5′-GAGAGGCCTACGGGGATCCAAGGAGATATAACAATGTACCCATACGATG TTCC-3′) and *Kpn*I-HA/cYFP-R, or from pBICp27-myc:nYFP using *Stu*I-myc/nYFP-F (5′-GGAGAGGCCTACGGGGATCCAAGGAGATATAACAATGGAGCAGAAGCT GATCAGC-3′) and *Kpn*I-myc/nYFP-R, respectively. The amplified DNA fragments were digested with *Stu*I and *Kpn*I, and inserted into *Stu*I/*Kpn*I-digested pBICp35 to construct pBICHA:cYFP and pBICmyc:nYFP.

(vii) pBICHA:cYFP-Hsp70 and pBICHA:cYFP-Hsp90. The sequence of HA-tagged cYFP was amplified from pBICHA-cYFP using *Stu*I-HA/cYFP-F and *Stu*I-HA/cYFP-R (5′-GTAGGCCTCTTGTACAGCTCGTCCATGCCGAG-3′). The amplified DNA was digested with *Stu*I, and cloned into *Stu*I-digested pBICHsp70 and pBICHsp90 to construct pBICHA-cYFP:Hsp70 and pBIC HA-cYFP:Hsp90.

(viii) pBICmyc:nYFP-Hsp70 and pBICmyc:nYFP-Hsp90. The sequence of myc-tagged nYFP was amplified from pBICmyc-nYFP using *Stu*I-myc/nYFP-F and *Stu*I-myc/nYFP-R (5′-GTAGGCCTGGCCATGATATAGACGTTGTGG-3′), respectively. The amplified DNA was digested with *Stu*I, and cloned into *Stu*I-digested pBICHsp70 to construct pBICHA-cYFP:Hsp70 and pBICmyc-nYFP:Hsp70.

(ix) pBICp27-HA:cYFP. The sequence of C-terminal half of YFP was amplified from pBI_C-CY using HA/cYFP-F

(5′-TACCCATACGATGTTCCTTACTTGTACAGCTCGTCCATG-3′) and *Kpn*I-HA/cYFP-R (5′-AGCGGGGTACCTTACTTGTACAGCTCGTCCATG-3′). A PCR fragment was then amplified from pBICp27 using p27-22R (5′-AGCAGATGGAACGTGTAG-3′) and HA/p27-R (5′-AGCGTAATCTGGAACATCGTATGGGTAAAAATCCTCAAGGGATTTGA-3′). Then, a recombinant PCR product was amplified from the mixture of these fragments using p27-22R and *Kpn*I-HA/cYFP-R, digested with *Eco*RI and *Kpn*I, and inserted into the corresponding region of pBICp27.

(x) pBICp27-myc:nYFP. The sequence of N-terminal half of YFP was amplified from pBI_C-NY using myc/nYFP-F (5′-GAGCAGAAGCTGATCAGCGAGGAGGACCTGGCCGGTGGTGGAGGAGCC GGC-3′) and *Kpn*I-myc/nYFP-R (5′-AGCGGGGTACCTTAGGCCATGATATAGACGTTG-3′). A PCR fragment was then amplified from pBICp27 using p27-22R and myc/p27-R (5′-CAGGTCCTCCTCGCTGATCAGCTTCTGCTCAAAATCCTCAAGGGATTTGA -3′). Then, a recombinant PCR product was amplified from the mixture of these fragments using p27-22R and *Kpn*I-myc/nYFP-R, digested with *Eco*RI and *Kpn*I, and inserted into the corresponding region of pBICp27.

(xi) pBICp88-HA:cYFP. The sequence of C-terminal half of YFP was amplified from pBI_C-CY using HA/cYFP-F and *Kpn*I/HA/cYFP-R, and a PCR fragment was amplified from pBICp88 using p88-167R (5′-AGTGCGAGCTTCGTTGG-3′) and HA/p88-R (5′-AGCGTAATCTGGAACATCGTATGGGTATCGGGCTTTGATTAGATCTTTG-3 ′). Then, a recombinant PCR product was amplified from the mixture of these fragments using p88-167R and *Kpn*I-HA/cYFP-R, digested with *Xho*I and *Kpn*I, and inserted into the corresponding region of pBICp88.

(xii) pBICp88-myc:nYFP. The sequence of N-terminal half of YFP was amplified from pBI_C-NY using myc:nYFP-F and *Kpn*I-myc/nYFP-R, and a PCR fragment was amplified from pBICp88 using p88-167R and myc/p88-R (5′-CAGGTCCTCCTCGCTGATCAGCTTCTGCTCTCGGGCTTTGATTAGATCTTTG-3′). Then, a recombinant PCR product was amplified from the mixture of these fragments using p88-167R and *Kpn*I-myc/nYFP-R, digested with *Xho*I and *Kpn*I, and inserted into the corresponding region of pBICp88.

(xiii) pBICsGFP-Hsp70 and pBICsGFP-Hsp90. The GFP sequence was amplified from pBICRMsG using *Stu*I-sGFP-F (5′-GGAGAGGCCTACGGGGATCCAAGGAGATATAACAATGGTGAGCAAGGGCGAGGAGCTG-3′) and *Stu*I-sGFP-R (5′-CCGTAGGCCTCTTGTACAGCTCGTCCATG-3′), digested with *Stu*I and inserted into *Stu*I-digested pBICHsp70 and pBICHsp90 to construct pBICsGFP-Hsp70 and pBICsGFP-Hsp90, respectively.

(xiv) pBICDRm-p27. A PCR fragment from pDsRed-monomer-Actin was amplified using Bam/DRm-F (5′-GGGGATCCGGATGGACAACACCGAGGACGTCATC-3′) and p27/DRm-R (5′-ATTTATAAAACCCATGCCCCCCTGGGAGCCGGAGTGGCGG-3′), and a PCR fragment from pUCR1 was amplified using DRm/p27-F (5′-CACTCCGGCTCCCAGGGGGGCATGGGTTTTATAAATCTTT-3′) and Kpn/p27-R (5′-GGGGTACCCTAAAAATCCTCAAGGGATTT-3′). Then, a recombinant PCR product was amplified from the mixture of these two fragments by the use of Bam/DRm-F and Kpn/p27-R, digested with *Bam*HI and *Kpn*I, and inserted into the corresponding region of pBICp35.

(xv) pBICp27-DRm. A PCR fragment from pBICp27 was amplified using p27-47R (5'-AGATGACATGGGAAAGG-3') and DRm-p27-R

(5′-CCATGCCCCCAAAATCCTCAAGGGATTTGA-3′), and a PCR fragment from pBICER-DRm (35) was amplified using p27-DRm-F (5′-TTTTGGGGGCATGGACAACACCGAGGACGT-3′) and *Kpn*I-DRm-R (5′-CGGGGTACCCTACTGGGAGCCGGAGTGGCGGG-3′). Then, a recombinant PCR product was amplified from the mixture of these two fragments by the use of p27-47R and *Kpn*I-DRm-R, digested with *Eco*RI and *Kpn*I, and inserted into the corresponding region of pBICp27.

(xvi) pUEGFP2. pBE2113-GUS (54) was cut with *Sac*I, treated with T4 DNA polymerase, cut with *Sma*I, and self-ligated to eliminate GUS gene. The small *Hin*dIII/*Eco*RI fragment of the resultant plasmid was inserted into the *Hin*dIII/*Eco*RI site of pUC118 (Takara Bio), creating pUC2113. A GFP gene was PCR-amplified from pBICB3aGFP (35) using the Xba/5LGFP5' primer (5'-GGTGGCTCTAGAAAGGAGATATAACAATGAGTAAAGGAGAAGAACT-3') and the Bam/GFP3' primer (5'-GGGGGGATCCTTATTTGTATAGTTCATCC-3'). The amplified fragment was cut with *Xba*I and *Bam*HI and inserted into the *Xba*I/*Bam*HI site of pUC2113, creating pUEGFP2.

(xvii) pUBp27-HA. A PCR fragment was amplified from pBICp27-HA using *BamH*I-p27-F (5′-GGAGAGGCCTACTCTAGAGGATCCGGATGGGTTTTATAAATCTT-3′) and *Kpn*I-p27-HA-R (5′-TTCAGCGGGGTACCCTAAGCGTAATCTGGAACATCGTATGGGTA-3′), digested with *BamH*I and *Kpn*I, and inserted into corresponding region of pUBP35.

(xviii) pUBp88-HA. The sequence of p88 was amplified from pUBp88 using p88-XhoI-F (5′-CCTGTCGATGTACTCGAGAAGGTGGCGTTT-3′) and p88-H*A*-R (5′- TTAAGCGTAATCTGGAACATCGTATGGGTATCGGGCTTTGATTA-3′). And a PCR fragment from pUBp88 was amplified using p88-HA-F

(5′-TACCCATACGATGTTCCAGATTACGCTTAAGGTACCCCGCTGAA -3′) and M13-rev (5′-CAGGAAACAGCTATGACCATG-3′). Then, a recombinant PCR product was amplified from the mixture of these fragments using p88-*Xho*I-F and M13-rev, digested with *Xho*I and *Kpn*I, and inserted into the corresponding region of pUBp88.

***In vitro* transcription.** The plasmids with the prefixes 'pUC' or 'pRC' were digested with *Sma*I. The linearized plasmids were used as templates for *in vitro* transcription by T7 RNA polymerase as described previously (58). If required, capped transcripts were prepared using the ScriptCap m^7G capping system according to the manufacturer's instruction (Epicentre Biotechnologies, Madison, WI).

Inhibitor treatments. 2-phenylethynesulfonamide (PES), Methanesulfonamide (MS), geldanamycin (GDA) and MG132 were purchased from EMD Biochemicals, Inc. (Gibbstown, NJ), Wako (Osaka, Japan), Sigma-Aldrich (St. Louis, MO), and Merck (Darmstadt, Germany), respectively. The inhibitors were diluted from stock solutions in dimethyl sulfoxide (DMSO) (Sigma-Aldrich). For the control experiments, an equivalent concentration of DMSO was applied.

Protoplast experiments. Protoplasts were prepared from tobacco BY-2 suspension cultured cell as described previously (84). BY-2 protoplasts (~3×10^5) were inoculated with *in vitro*-transcribed RNA1 and RNA2 (1 μg each), or with RCNMV virion (2 μg), or with pUBRC1 and pUBRC2 (5 μg each), or with pUBp27-HA, pUBp88-HA, and *in vitro*-transcribed RNA2 (10 μg, 5 μg, and 500 ng, respectively) as described previously (21). The inoculated protoplasts were incubated at 17 °C for 16 h in the presence of PES, MS, or GDA. Viral RNAs were detected by northern blotting.

***Agrobacterium* infiltration.** The plasmids containing the prefixes 'pBIC' and 'pTV' were introduced by electroporation into *Agrobacterium tumefaciens* GV3101 (pMP90) and *A. tumefaciens* GV3101 (pSoup), respectively. *Agrobacterium* suspensions were mixed at a final OD_{600} of 0.2 each for Bimolecular fluorescence

complementation (BiFC) experiments, OD_{600} of 0.4 each for subcellular localization assays, and OD_{600} of 0.5 for gene silencing. *Agrobacterium* suspensions harboring an empty vector, pBICp35, were used as the filler. The mixtures were infiltrated into *N. benthamiana* leaves essentially as described by Takeda *et al*. (84).

Silencing of *Hsp70* and *Hsp90* in *N. benthamiana* plants. Appropriate combinations of silencing vectors were expressed by *Agrobacterium* infiltration in 3- to 4-weeks-old *N. benthamiana* plants as described previously (73). At 10 days post agroinfiltration (dai), the leaves above the agroinfiltrated leaves were inoculated with *in vitro* transcribed RNA1 and RNA2. The inoculated plants were incubated at 22 °C for 2 days. Total RNAs were extracted using TRIzol reagent (Invitrogen), treated with RQ1 RNase-free DNase (Promega, Madison, WI), purified by phenol/chloroform and chloroform extractions and precipitated with ethanol. Viral RNAs were detected by northern blotting. The mRNA levels of *NbHsp70c-1* (6, 38) were examined by semiquantitative RT-PCR using Nb70c-F (5′-CTAGAATCCCAAAGGTGCAACAGC-3′) and Nb70c-R (5′-CTTCTCATCTTTCACAGTGTTCCTC-3′). The mRNA levels of *NbHsp90* were examined as described previously (85). As a control to show the equal amounts of complementary DNA templates in each reaction, ribulose 1,5-biphosphate carboxylase small subunit gene (*RbcS*), a constitutively expressed gene, was amplified by RT-PCR using NbRbcS-F (5′-CCTCTGCAGTTGCCACC-3′) and NbRbcS-R (5′-CCTGTGGGTATGCCTTCTTC-3′).

BiFC and subcellular localization assays. Appropriate combinations of Yellow fluorescent protein (YFP) fragments-fused proteins or fluorescent protein-fused proteins were expressed in *N. benthamiana* leaves by *Agrobacterium* infiltration. Fluorescence of, YFP, green fluorescent protein (GFP), DsRed monomer (DRm), and mCherry were visualized with confocal microscopy at 3 days post infiltration (dpi) for subcellular

localization assay and at 4 dpi for BiFC. Protein expression was confirmed by western blotting. Accumulations of viral RNAs were analyzed by northern blotting.

Confocal microscopy. The fluorescence signals of GFP, YFP, DRm, and mCherry were observed using an Olympus FluoView FV500 confocal microscope (Olympus Optical Co., Tokyo, Japan) equipped with an argon laser, a He:Ne laser, and a 40× Plan Apo oil immersion objective lens. The samples were excited with the argon laser for GFP/YFP, and with the He:Ne laser for DsRed-monomer/mCherry. We used a dichroic mirror, DM488/543, a beam splitter, SDM560, and two emission filters, BA505-525 for GFP/YFP, and BA560IF for DsRed-monomer/mCherry. Scanning was performed in sequential mode to minimize signal bleed-through. Images were processed using Adobe Photoshop CS3 software.

Glutathione S-transferase (GST) pull-down assays. *E. coli* Rossetta 2 (DE3) (Invitrogen) transformed by pET42a, pET42a-Hsp70 or pET42a-Hsp90 was grown overnight at 37 °C in LB medium containing kanamycin (100 μg/ml). The overnight cultures of the transformed *E. coli* were diluted to1:50 in LB medium containing kanamycin (100 μg/ml). After incubation for 2h at 37 °C, protein expression was induced by the addition of 0.3 mM isopropyl-β-D-thiogalactopyranoside. The cells expressing GST, GST-Hsp70 or GSR-Hsp90 were cultured at 28 °C for 1 h, 4h or 4h, respectively. The induced cells were harvested by centrifugation at 5,000×g for 5 min.

Cells collected from 5 ml (pET-42a) and 10 ml (pET42a-Hsp70 and pET42a-Hsp90) of medium were resuspended in 500 μl of phosphate buffer saline (140 mM NaCl, 2.7 mM KCl, 10 mM Na_2HPO_4, and 1.8 mM KH_2PO_4), and sonicated on ice to disrupt the cells. After sonication, Triton-X 100 was added at the final concentration of 0.5% and centrifuged at 15,000×g for 10 min at 4°C. The supernatant was added to 12.5 μl bed volume of equilibrated Glutathione Sepharose 4B (GE Healthcare, Little Chalfont, Buckinghamshire, UK), and incubated at 4°C for 1 h with gentle rotation. The resin was

washed three times with 1 ml of binding buffer (50 mM Tris-HCl pH 7.4, 150 mM NaCl, 10 mM 2-mercaptoethanol, and 0.5% Triton X-100). After washing, the resin was incubated for 2 h at 4°C in 200 μl of binding buffer containing 500 ng of the purified His-p27-FLAG (52). After incubation, the resin was washed three times with 500 μl of binding buffer. The bound proteins were eluted by addition of Laemmli sample buffer (42), followed by incubation for 3 min at 95°C. Protein samples were subjected to SDS–PAGE and then blotted onto a PVDF membrane. The separated proteins were analyzed by western blotting, and stained with Ponceau S.

Cell-free *in vitro* translation and replication experiments. The cell extracts of evacuolated BY-2 protoplasts (BYL) were prepared and the *in vitro* translation/replication reactions were performed essentially as described previously (28, 40, 52, 53). BN–PAGE analysis was performed as described previously (53), except that the total protein samples solubilized with 0.5% Triton X-100 were subjected to BN-PAGE. StreptoTag affinity purification was performed essentially as described previously (27). Immunopurification of p27-FLAG is described below.

Immunopurification of p27-FLAG. p27-FLAG was expressed in BYL by adding an *in vitro* transcript to a concentration of 20 nM. After 2 h of incubation, BYL expressing p27-FLAG was incubated on ice for 30 min with 500 μM of PES, MS or GDA. At this time, ADPβS or ATPγS, which stabilizes the binding of Hsp70 or Hsp90 to substrate proteins, respectively, was also added to concentrations of 2 mM. Then, 10 μl bed volume of ANTI-FLAG M2-Agarose Affinity Gel (Sigma-Aldrich) was added to the BYL and further incubated for 90 min with occasional mixing. The resin was washed three times with 200 μl of TR buffer (40) supplemented with 500 mM NaCl and 0.1% Triton-X-100 for the analysis of p27–Hsp70 interaction, or with TR buffer supplemented with 0.1% Triton X-100 for the analysis of p27–Hsp90 interaction. The bound proteins were eluted by addition of Laemmli sample buffer, followed by

incubation for 3 min at 95°C. Protein samples were subjected to SDS-PAGE, followed by western blotting with appropriate antibodies.

Northern blot analysis. Northern blot analysis was performed essentially as previously described (28). The digoxigenin-labelled RNA probes specific for the 3′ untranslated regions (UTRs) of RCNMV RNA1 and RNA2, and the full-length negative-strand RNA1 and RNA2 were described previously (56, 57). The RNA signals were detected with a luminescent-image analyzer (LAS-1000 plus; Fuji Photo Film, Japan), and the signal intensities were quantified using the NIH Image program.

Western blot analysis. Western blot analysis was performed essentially as described previously (53). Protein samples were subjected to SDS-PAGE or BN-PAGE and transferred to polyvinylidene difluoride (PVDF) membranes (Immobilon-P, Millipore, Bedford, MA). Anti-p27 rabbit polyclonal antibody (84), anti-NtHsp90 rabbit polyclonal antibody (82), anti-Hsp70/Hsc70 mouse monoclonal antibody (Stressgen, Victoria, BC, Canada), anti-c-myc mouse polyclonal antibody (Santa Cruz Biotechnology Inc., Santa Cruz, CA), anti-HA rat monoclonal antibody (Roche Diagnostics, Penzberg, Germany), and anti-FLAG M2 mouse monoclonal antibody (Sigma-Aldrich) were used as the primary antibodies. Alkaline phosphatase (AP)-conjugated anti-rabbit IgG antibody (Cell Signaling Technology, Beverley, MA), AP-conjugated anti-mouse IgG antibody (KPL, Gaithersburg, MD), AP-conjugated anti-rat IgG antibody (Santa Cruz Biotechnology Inc.), horseradish peroxidase (HRP)-conjugated anti-rabbit IgG antibody (Cell Signaling Technology), and HRP-conjugated anti-mouse IgG antibody (KPL) were used as the secondary antibodies. To detect p88-T7, AP-conjugated anti-T7 monoclonal antibody (Merck) was used. Signals were detected using a luminescent-image analyzer (LAS-1000 plus), and the signal intensities were quantified using the NIH Image program.

Accession numbers. The GenBank accession numbers for the *Nicotiana tabacum*

Hsp70 and Hsp90 cDNA sequences reported in this paper are AB689673 and AB689674, respectively.

RESULTS

Hsp70 and Hsp90 are host factors required for RCNMV RNA replication. In a previous study, we identified many host proteins that were co-purified with RCNMV replicase complexes from virus-infected *Nicotiana benthamiana* tissues. These included Hsp70- and Hsp90-related proteins (53). This led us to investigate whether Hsp70 and Hsp90 are involved in RCNMV infection. We applied *Tobacco rattle virus* (TRV)-based gene silencing to downregulate cytosolic *Hsp70* and *Hsp90* in *N. benthamiana* plants. The TRV vectors harboring the partial fragment of *Hsp70* (TRV:Hsp70) (38) or *Hsp90* (TRV:Hsp90) (85) were expressed by *Agrobacterium*-mediated expression. As a control, the empty TRV vector (TRV:00) (73) was expressed. The newly developed leaves were inoculated with *in vitro* transcribed RCNMV RNA1 and RNA2 at 10dai. Note that any morphological defects such as chlorotic and stunted phenotypes were not observed at this stage (Fig.1A), although such phenotypes became visible after 16 dpi (data not shown). Total RNA was extracted from the inoculated leaves two days after inoculation (at 12 dpi). Semiquantitative RT-PCR analysis confirmed the specific reduction of *Hsp70* and *Hsp90* mRNAs in plants infiltrated with TRV:Hsp70 and TRV:Hsp90, respectively (Fig. 1A and B, lower panels). Importantly, the accumulation of RCNMV RNAs was impaired in *Hsp70*- and *Hsp90*-silenced plants as assessed by northern blotting (Fig. 1A and B, upper panels). These results suggest that Hsp70 and Hsp90 play positive roles during RCNMV infection.

To test whether Hsp70 and Hsp90 function in RCNMV RNA replication in a single cell, we treated tobacco BY-2 protoplasts with specific inhibitors of Hsp70 or Hsp90, PES or GDA, respectively. These inhibitors have been used successfully to analyze the functions of Hsp70 and Hsp90 in plant and animal systems (22, 23, 31, 43, 44, 82). MS, an analogue of PES, was used as a negative control for PES. Protoplasts inoculated with

in vitro transcribed RNA1 and RNA2 were incubated in the presence of various amounts of the inhibitors. Northern blot analysis showed that PES had an inhibitory effect on the accumulation of RCNMV RNAs; 40 μM of PES inhibited viral RNA accumulation by about 95%, but MS had no effect (Fig. 2A and B). GDA had little effect on the accumulation of RCNMV RNAs (data not shown). However, GDA inhibited viral RNA accumulation when protoplasts were inoculated with the plasmids that transcribe RCNMV RNAs under the control of *Cauliflower mosaic virus* 35S promoter: 50 μM of GDA inhibited the accumulation of RCNMV RNAs by about 70% (Fig. 2C and D). Importantly, GDA did not reduce the accumulation of GFP mRNAs (Fig. 2C), indicating that the reduction of viral RNA accumulations was not caused by the inhibitory effect of GDA on CaMV 35S promoter-driven transcription under the assay condition. The inhibitory effect of GDA on viral RNA accumulations was also observed in protoplasts inoculated with RCNMV virionS (Fig. 2E and F). Overall, these data suggest that both Hsp70 and Hsp90 are required for RCNMV RNA replication in a single cell.

Hsp70 and Hsp90 interact with p27 within the virus-induced aggregated structures of the ER in the context of viral RNA replication. Because Hsp70 and Hsp90 are well-known protein chaperones, these chaperones might bind directly or indirectly to p27 or p88 or both. To characterize these interactions in living cells, we used a BiFC assay . We isolated cDNAs encoding Hsp70 and Hsp90 were isolated from tobacco BY-2 cultured cells as described in Materials and Methods. We first tested whether p27 interacts with Hsp70 and Hsp90. p27 fused to the N- or C-terminal half of YFP at the C-terminus was expressed together with Hsp70 or Hsp90 fused to the other halves of YFP at the N-terminus (e.g., p27-nYFP plus cYFP-Hsp70 or cYFP-Hsp90, p27-cYFP plus nYFP-Hsp70 or nYFP-Hsp90) in the presence of p88, RNA2, mCherry containing an ER targeting signal (ER-mCherry) (34), and the silencing suppressor p19

of *Tomato bushy stunt virus* (TBSV) in *N. benthamiana* by *Agrobacterium* infiltration. At 4dai, large aggregated fluorescent structures of YFP were detected (Fig. 3A and B, left panels). This YFP fluorescence was merged with the large aggregated fluorescent structures of ER-mCherry (Fig. 3A and B, middle and right panels), a characteristic feature of morphological changes of ER induced by RCNMV infection (88) (Kusumawanegara *et al*., in press). Little or no YFP fluorescence was detected in control experiments, in which YFP fragments, p27, Hsp70, or Hsp90 were expressed separately instead of their fusion protein counterparts (Fig. 3C and D). Western blot analysis confirmed the accumulation of YFP fragment-fused proteins in *Agrobacterium*-infiltrated leaves (Fig. 3E and F). Northern blot analysis showed that p27-cYFP but not p27-nYFP supported the accumulation of positive- and negative-strand RNA2 (Fig. 3E and F), indicating that p27-cYFP participated in the replication of RNA2 under the assay conditions. Together, these results suggest that p27 interacts with Hsp70 and Hsp90 *in planta* in the absence and presence of viral RNA replication.

We also used BiFC to test whether p88 interacts with Hsp70 and Hsp90, but we failed to observe these interactions. Appropriate expression of C-terminally YFP fragment-fused p88 in combination with the other YFP fragment-fused Hsp70 or Hsp90 showed no or little YFP fluorescence (data not shown). We note that both p88 derivatives were functional in supporting the replication of RNA2, although C-terminally cYFP-fused p88 did not accumulate to detectable levels (data not shown). Thus, it appears that the interactions of p88 with Hsp70 and Hsp90 do not occur, or, if they occur, the interactions are too weak to be detected by BiFC.

Because the reconstitution of YFP is irreversible (49), the above BiFC experiments did not rule out the possibility that the reconstitution of YFP occurred only in the cytoplasm, and that the YFP signals detected in the aggregated ER structures reflected

artificial tethering of Hsp70 and Hsp90 to p27 localized to the ER. To check whether Hsp70 and Hsp90 co-localize with p27 without the artificial tethering, we first examined the subcellular localization of Hsp70 and Hsp90 in the absence of RCNMV infection by expressing GFP-fused Hsp70 (GFP-Hsp70) or Hsp90 (GFP-Hsp90) together with ER-mCherry in *N. benthamiana*. At 3dai, fluorescence of GFP-Hsp70 and GFP-Hsp90 was observed in the nucleus and cytoplasm (Fig. 4A and C, left panels). Fluorescence of ER-mCherry showed an ER distribution that included the nuclear envelope (Fig. 4A and C, middle panels). The fluorescence of GFP-Hsp70 and GFP-Hsp90 was merged only partially with the fluorescence of ER-mCherry (Fig. 4A and C, right panels), indicating that Hsp70 and Hsp90 hardly localized to the ER in the absence of RCNMV infection. However, when co-expressed with C-terminally DRm-fused p27 (p27-DRm), p88, and RNA2, the large aggregated fluorescence of GFP-Hsp70 and GFP-Hsp90 was detected in addition to the cytoplasmic and nuclear fluorescence (Fig. 4B and D, left panels), and it merged with the fluorescent aggregates of p27-DRm (Fig. 4B and D, middle and right panels). These results show that GFP-Hsp70 and GFP-Hsp90 co-localized with p27-DRm in the large aggregated structures of the ER. We note that the p27-DRm was functional in supporting the replication of RNA2 (data not shown). Together, these data suggest that Hsp70 and Hsp90 are recruited by p27 to the large aggregate structures of the ER in the context of viral RNA replication.

We used an *in vitro* GST pull-down assay to characterize further the interactions of p27 with Hsp70 and Hsp90. We purified p27 with an N-terminal His-tag and a C-terminal FLAG-tag (His-p27-FLAG), as described previously (52). N-terminally GST-fused Hsp70 (GST-Hsp70) or Hsp90 (GST-Hsp90) captured on glutathione-bound beads was incubated with purified His-p27-FLAG. After extensive washing, the bound proteins were analyzed by western blotting with an anti-FLAG antibody.

His-p27-FLAG was pulled down by both GST-Hsp70 and GST-Hsp90, but not by GST alone, which was used as a negative control (Fig. 5A). Thus, like other substrate proteins, Hsp70 and Hsp90 bind to p27 via protein–protein contacts.

Hsp70 and Hsp90 promote the assembly of the 480-kDa replicase complex of RCNMV by binding to p27. Because PES and GDA block interactions of Hsp70 and Hsp90 with their client proteins, respectively (23, 31, 43, 44), we hypothesized that these chemicals inhibit RCNMV RNA replication by blocking the interactions of Hsp70 and Hsp90 with p27. To test this, we used BYL, an *in vitro* translation/replication system (40). BYL has been used successfully to recapitulate the RNA replication processes of RCNMV (1, 21, 27-29, 52, 53, 57, 74, 81). We first tested the effects of PES and GDA on the interactions of p27 with Hsp70 and Hsp90, respectively. BYL expressing C-terminally FLAG-tagged p27 (p27-FLAG), which is functional in RCNMV RNA replication (53), was subjected to immunopurification with anti-FLAG antibodies in the presence of inhibitors. Western blot analysis showed that PES and GDA blocked the co-purification of endogenous Hsp70 and Hsp90 with p27-FLAG, respectively (Fig. 5B and C). These results confirmed the inhibitory effects of PES and GDA on the interactions of p27 with Hsp70 and Hsp90, respectively.

Next, we tested the effects of PES and GDA on the negative-strand RNA synthesis of RCNMV RNAs. Both chemicals inhibited the accumulation of p27 and negative-strand RNAs in BYL (Fig. 6), suggesting that Hsp70 and Hsp90 are required for the translation/accumulation of p27 protein as well as the negative-strand RNA synthesis. We then designed an assay using BYL to investigate the roles of Hsp70 and Hsp90 in RCNMV RNA replication other than in protein translation and folding (Fig. 7A). This assay is based on the replication mechanism of RNA2 that exploits p27 and p88 supplied *in trans* in contrast to the translation-coupled replication of RNA1 (27, 66). This assay enabled us to monitor the assembly of the 480-kDa replicase complex and

the subsequent negative-strand synthesis of RNA2 after the completion of translation and folding of p27 and p88 proteins. In this assay, p27-FLAG and C-terminally T7-tagged p88 (p88-T7) were translated individually in BYL. These BYL were mixed together following the addition of the protein synthesis inhibitor cycloheximide. RNA2 was then added with PES or GDA to the mixed BYL, followed by further incubation. Northern blot analysis showed dose-dependent inhibition of the negative-strand RNA2 synthesis by PES and GDA (Fig. 7B, E and F). Western blot analysis on the protein complexes separated by BN-PAGE revealed that PES and GDA inhibited the formation of the 480-kDa replicase complex in a dose-dependent manner (Fig. 7B-D). Interestingly, PES but not GDA increased the accumulation of large complexes (~1024 kDa) (Fig. 7B-D). MS had no effects on the accumulation of the 480-kDa complexes and negative-strand RNA2 (Fig. 7B). PES affected the stability of p88-T7 (Fig. 7B-C). However, this reduction in p88-T7 was not the major reason for the inhibitory effect of PES on the negative-strand synthesis of RNA2 because more negative-strand RNA2 accumulated in the presence of MS than in the presence of PES even when the amount of p88-T7 in MS-treated BYL was adjusted to be similar to or even less than that of PES-treated BYL (Fig. 7G). Taken together, these results suggest that Hsp70 and Hsp90 facilitate the assembly of RCNMV replicase complex likely through interactions with p27 and thereby promote subsequent negative-strand RNA synthesis.

Hsp90 regulates the assembly of the 480-kDa replicase complex by promoting the specific binding of p27 to YRE. We have shown previously that the addition of RNA2 increases the accumulation of the 480-kDa complexes in BYL (53) and that mutations in p27 that compromise the binding activity of p27 to YRE of RNA2 affect the assembly of the 480-kDa complexes in BYL (21). An aptamer-based pull-down assay using p27 produced in BYL showed the interaction between p27 and YRE, whereas no such interaction was observed using purified recombinant p27 produced in

Escherichia coli in an electrophoretic mobility shift assay (27), suggesting that an unknown plant factor(s) is required for the binding of p27 to YRE. These findings led us to hypothesize that the interaction between p27 and YRE is a key step in the assembly of the 480-kDa replicase complex on RNA2 and that this step is regulated by Hsp70 and/or Hsp90.

To test this hypothesis, we first used an RNA2 mutant (RNA2 LM8) that is unable to interact with p27 (27) to evaluate its ability to support the assembly of the 480-kDa complex. After addition of cycloheximide, BYL expressing p27-FLAG was mixed with BYL expressing p88-T7, as illustrated in Fig. 7A. Wild-type RNA2 or RNA2 LM8 was then added to the mixed BYL, followed by further incubation. Northern blot analysis confirmed the requirement of p27-YRE interaction for the negative-strand synthesis of RNA2 (Fig. 8A) (1, 21, 27). Western blot analysis in combination with BN-PAGE showed that the accumulation of the 480-kDa complex was increased by the addition of wild-type RNA2, whereas little increase in the accumulation of the 480-kDa complex was observed when RNA2 LM8 was added (Fig. 8A). These results indicate that the binding of p27 to YRE is one of the key steps for the assembly of the 480-kDa replicase complex.

We next used a pull-down assay based on the high affinity of an RNA aptamer termed 'STagT' with streptomycin to test the effects of PES and GDA on the interaction between p27 and YRE (2, 9). This RNA-based pull-down assay in combination with the membrane-depleted BYL (BYLS20), which can support negative-strand synthesis of RCNMV RNAs, was used to analyze the interaction between p27 and YRE (21, 27). STagT-fused YRE was incubated with BYLS20 expressing p27-FLAG in the presence of the inhibitors. The p27-FLAG proteins interacting with STagT-fused YRE were pulled down by streptomycin-conjugated beads. Similar amounts of bait RNAs were purified and indicated by ethidium bromide staining. Interestingly, western blotting with

anti-FLAG antibodies showed that GDA but not PES inhibited the co-purification of p27-FLAG with STagT-fused YRE (Fig. 8B). These results suggest that the interaction of p27 with Hsp90, but not with Hsp70, is critical for the interaction between p27 and YRE of RNA2, which then promotes the formation of the 480-kDa replicase complex. These results also illustrate the differential contributions of Hsp70 and Hsp90 in the assembly of the 480-kDa replicase complex.

DISCUSSION

In this study, we showed that Hsp70 and Hsp90 play critical roles in different steps of the assembly of the RCNMV replicase complex likely through interactions with p27. Inhibition of the p27–Hsp70 interaction resulted in the assembly of p27 into large complexes that were nonfunctional in viral RNA synthesis. By contrast, inhibition of p27–Hsp90 interaction lost the ability of p27 to bind to viral genomic RNA2, which is critical for the assembly of the 480-kDa replicase complex. These findings reveal the regulatory mechanism for the assembly of viral replicase complexes and suggest the potential roles of Hsp70 and Hsp90 in controlling the assembly of ribonucleoprotein complexes.

Hsp70 regulates the correct assembly of the RCNMV replicase complex. Hsp70 interacts with viral replicase proteins of various eukaryotic positive-strand RNA viruses (5, 11, 64, 91). For example, Pogany *et al*. (71) successfully reconstituted the RdRP activities of TBSV replicase complexes using viral replicase proteins, p33 and p92, produced in *E. coli* with the membrane fractions of yeast extracts and purified yeast Hsp70. They suggested that Hsp70 plays an integral role in the early replication process of TBSV, including the assembly of TBSV replicase complexes.

In the present study, we analyzed the assembled RCNMV replicase complex itself and found that inhibition of p27–Hsp70 interaction by PES causes the formation of

large aggregates containing p27 and reduces accumulation of the 480-kDa replicase complex, which in turn impairs viral RNA synthesis (Fig. 7). These data lead us to propose that one of the major roles of Hsp70 in viral RNA replication is to control the proper assembly of viral replicase complexes.

How does Hsp70 regulate the assembly of the RCNMV replicase complex? Based on the accumulation of nonfunctional large complexes upon the inhibition of p27–Hsp70 interaction, it is possible that the Hsp70 prevents the aggregation of p27 protein and thereby facilitate the assembly of the RCNMV relicase complex. In fact, it has been reported that Hsp70 family proteins promote the assembly of cellular multiprotein complexes such as immunoglobulin G antibody and synaptic SNARE complex by preventing aggregations of their component proteins (13, 75). Alternatively, the large complexes could be intermediates for the assembly of the RCNMV replicase complex and Hsp70 might assist the assembly process from these complexes to functional replicase complexes. Such functions are reported for the chaperones dedicated to the assembly of proteasome (60). Further studies are needed to gain mechanistic insights into how Hsp70 regulates the assembly of RCNMV replicase complex.

Hsp90 regulates the key interaction between p27 and YRE, which is required for the assembly of the RCNMV replicase complex. Gene silencing in plants and pharmacological inhibition in protoplasts showed that Hsp70 and Hsp90 are host factors required for RCNMV replication (Figs. 1 and 2). Interestingly, however, an inhibitory effect of GDA in protoplast experiments was observed when RCNMV RNAs were supplied from plasmids or virions but not when *in vitro* synthesized RCNMV RNAs were directly introduced (Fig. 2C-F and data not shown). These results suggest that Hsp90 is required for plasmid or virion-dependent processes such as efficient transcription and virion uncoating. An alternative, but not mutually exclusive

interpretation is that Hsp90 plays a role in a very early step in the RCNMV replication process because time required for transcription from plasmids or virion uncoating must delay the initiation of viral RNA replication. The latter interpretation was supported by the finding that GDA inhibits two distinct steps in the early replication process of RCNMV *in vitro* (Figs. 6-8). The first step is the accumulation of p27 protein (Fig. 5). Inhibitory effect of GDA on p27 accumulation as well as viral RNA accumulation was also observed when BY-2 protoplasts were inoculated with plasmids that express hemagglutinin (HA)-tagged p27 and p88 together with RNA2 (data not shown). The roles of Hsp90 in the accumulation of RCNMV replicase proteins are discussed later. The second step is the binding of p27 to YRE of RNA2, which is a critical step in the assembly of the 480-kDa replicase complex (Fig. 8). A similar mode of assembly was proposed for TBSV replicase complexes: p33 auxiliary protein interacts with the internal replication element (IRE) located in the coding region of p92 RdRP (72), and this interaction is required for the RdRP activities of the TBSV replicase complexes in yeast and its cell-free extracts (70-72). However, unlike p27, p33 can bind to the IRE without other viral and host proteins (72). Thus, it appears that these two related viruses have evolved different strategies for the interactions of viral replicase proteins with replication templates and subsequent assembly of the viral replicase complexes.

Recently, Huang *et al*., (20) showed that Hsp90 of *N. benthamiana* binds to the 3′UTR of BaMV genomic RNA and is required for the efficient accumulation of the genomic RNA during the early stages of infection. This finding suggests a potential function of Hsp90 in regulating viral RNA replication through interaction with viral RNAs. However, it is unlikely that Hsp90 promotes the assembly of 480-kDa replicase complex by binding to RCNMV RNA2, because we failed to detect any interactions between Hsp90 and RNA2 in BYL based on StagT-aptamer pull-down assays (data not shown). It is still possible that Hsp90 binds to RNA1 as well as p27 and/or p88, which

may facilitate translation and subsequent assembly of the replicase complex. Interestingly, Lsm1-7 complex, which is involved in mRNA degradation in Processing Bodies, is required for translation and replication of *Brome mosaic virus* (BMV) genomic RNAs in yeast (3, 50, 65). Lsm1-7 complex binds directly to tRNA-like structures and the intergenic region of BMV RNA3 (14).

Roles of Hsp70 and Hsp90 in the translation/stability of RCNMV replicase proteins. PES and GDA decreased the accumulation of p27 in BYL when the inhibitors were present throughout the experiments (Fig. 6). However, the deleterious effects were not observed when these inhibitors were added after the addition of cycloheximide (Fig. 7B to D), suggesting that Hsp70 and Hsp90 are dispensable for the stability of p27 after translation. It is likely that Hsp70 and Hsp90 promote the synthesis of p27 as seen for the synthesis of flock house virus protein A (4, 92). Alternatively, it is possible that the translating p27 is protected from degradation by a ribosome-associated chaperone system, in which Hsp70 is thought to interact directly with nascent polypeptides emerging from ribosomes (37, 93). Co-translational binding of Hsp70 and/or Hsp90 might facilitate the subsequent function of these chaperones during the assembly of the RCNMV replicase complex.

By contrast, PES decreased the stability of p88 in BYL (Fig. 7B and D). The proteasome inhibitor MG132 did not restore the stability of p88 (data not shown), suggesting that Hsp70 might protect p88 from proteasome-independent degradation. However, it is also possible that the effect of PES on the stability of p88 is an artifact of the *in vitro* condition, in which p88 tends to form aggregates because of its overexpression (53). This situation never occurs during the actual infection process of RCNMV because p88 is translated by a programmed −1 ribosomal frameshifting at a quite low frequency (39, 81) and because the translation and accumulation of p88 are tightly coupled to viral RNA replication (27, 53, 66).

In conclusion, this study has demonstrated the multiple roles of Hsp70 and Hsp90 in the early replication process of RCNMV. These chaperones promote the translation of p27 and interact directly with p27. These interactions lead to the recruitment of Hsp70, Hsp90, and RNA2 to the ER membrane (Figs. 3, 4 and 8) (21, 27), where Hsp70 and Hsp90 regulate the assembly of the 480-kDa replicase complex (Figs. 7 and 8). Finally, the properly assembled 480-kDa replicase complex initiates viral RNA replication via complementary RNA synthesis (53).

ACKNOWLEDGEMENTS

The authors thank Dr. Ryohei Terauchi for pPVX.NbHsp70c-1, Dr. Takashi Araki for BiFC constructs, Drs. Ichiro Mitsuhara and Yuko Ohashi for the anti-NtHsp90 antibody and pBE2113-GUS, and Dr. David C. Baulcombe for TRV vectors. The authors are also grateful to Dr. Hiro-oki Iwakawa for helpful discussion. This work was supported in part by Grants-in-Aid for Scientific Research (A) (22248002) from the Japan Society for the Promotion of Science.

REFERENCES

1. **An, M. N., H. Iwakawa, A. Mine, M. Kaido, K. Mise, and T. Okuno.** 2010. A Y-shaped RNA structure in the 3' untranslated region together with the trans-activator and core promoter of *Red clover necrotic mosaic virus* RNA2 is required for its negative-strand RNA synthesis. Virology **405:**100-109.
2. **Bachler, M., R. Schroeder, and U. von Ahsen.** 1999. StreptoTag: A novel method for the isolation of RNA-binding proteins. RNA **5:**1509-1516.
3. **Beckham, C. J., H. R. Light, T. A. Nissan, P. Ahlquist, R. Parker, and A. Noueiry.** 2007. Interactions between brome mosaic virus RNAs and cytoplasmic processing bodies. J. Virol. **81:**9759-9768.

4. **Castorena, K. M., S. A. Weeks, K. A. Stapleford, A. M. Cadwallader, and D. J. Miller.** 2007. A functional heat shock protein 90 chaperone is essential for efficient flock house virus RNA polymerase synthesis in Drosophila cells. J. Virol. **81:**8412-8420.

5. **Chen, Y. J., Y. H. Chen, L. P. Chow, Y. H. Tsai, P. H. Chen, C. Y. F. Huang, W. T. Chen, and L. H. Hwang.** 2010. Heat shock protein 72 is associated with the Hepatitis C virus replicase complex and enhances viral RNA replication. J. Biol. Chem. **285:**28183-28190.

6. **Chen, Z. R., T. Zhou, X. H. Wu, Y. G. Hong, Z. F. Fan, and H. F. Li.** 2008. Influence of cytoplasmic heat shock protein 70 on viral infection of Nicotiana benthamiana. Mol. Plant Pathol. **9:**809-817.

7. **Chromy, L. R., J. M. Pipas, and R. L. Garcea.** 2003. Chaperone-mediated in vitro assembly of Polyomavirus capsids. Proc. Natl. Acad. Sci. U. S. A. **100:**10477-10482.

8. **Connor, J. H., M. O. McKenzie, G. D. Parks, and D. S. Lyles.** 2007. Antiviral activity and RNA polyinerase degradation following Hsp90 inhibition in a range of negative strand viruses. Virology **362:**109-119.

9. **Dangerfield, J. A., N. Windbichler, B. Salmons, W. H. Gunzburg, and R. Schroder.** 2006. Enhancement of the StreptoTag method for isolation of endogenously expressed proteins with complex RNA binding targets. Electrophoresis **27:**1874-1877.

10. **den Boon, J. A., A. Diaz, and P. Ahlquist.** 2010. Cytoplasmic viral replication complexes. Cell Host Microbe **8:**77-85.

11. **Dufresne, P. J., K. Thivierge, S. Cotton, C. Beauchemin, C. Ide, E. Ubalijoro, J. F. Laliberte, and M. G. Fortin.** 2008. Heat shock 70 protein interaction with Turnip mosaic virus RNA-dependent RNA polymerase within

virus-induced membrane vesicles. Virology **374:**217-227.

12. **Ellis, R. J.** 2006. Molecular chaperones: assisting assembly in addition to folding. Trends in Biochemical Sciences **31:**395-401.

13. **Feige, M. J., S. Groscurth, M. Marcinowski, Y. Shimizu, H. Kessler, L. M. Hendershot, and J. Buchner.** 2009. An unfolded C(H)1 domain controls the assembly and secretion of IgG antibodies. Mol. Cell **34:**569-579.

14. **Galao, R. P., A. Chari, I. Alves-Rodrigues, D. Lobao, A. Mas, C. Kambach, U. Fischer, and J. Diez.** 2010. LSm1-7 complexes bind to specific sites in viral RNA genomes and regulate their translation and replication. RNA **16:**817-827.

15. **Gamarnik, A. V., and R. Andino.** 1998. Switch from translation to RNA replication in a positive-stranded RNA virus. Genes Dev. **12:**2293-2304.

16. **Grad, W., and D. Picard.** 2007. The glucocorticoid responses are shaped by molecular chaperones. Mol. Cell. Endocrinol. **275:**2-12.

17. **Hafren, A., D. Hofius, G. Ronnholm, U. Sonnewald, and K. Makinen.** 2010. HSP70 and its cochaperone CPIP promote potyvirus infection in *Nicotiana benthamiana* by regulating viral coat protein functions. Plant Cell **22:**523-535.

18. **Hartl, F. U., A. Bracher, and M. Hayer-Hartl.** 2011. Molecular chaperones in protein folding and proteostasis. Nature **475:**324-332.

19. **Hsu, N. Y., O. Ilnytska, G. Belov, M. Santiana, Y. H. Chen, P. M. Takvorian, C. Pau, H. van der Schaar, N. Kaushik-Basu, T. Balla, C. E. Cameron, E. Ehrenfeld, F. J. M. van Kuppeveld, and N. Altan-Bonnet.** 2010. Viral reorganization of the secretory pathway generates distinct organelles for RNA replication. Cell **141:**799-811.

20. **Huang, Y. W., C. C. Hu, M. R. Liou, B. Y. Chang, C. H. Tsai, M. Meng, N. S. Lin, and Y. H. Hsu.** 2012. Hsp90 interacts specifically with viral RNA and differentially regulates replication initiation of Bamboo mosaic virus and

associated satellite RNA. PLoS Pathog . **8:**e1002726.

21. **Hyodo, K., A. Mine, H. Iwakawa, M. Kaido, K. Mise, and T. Okuno.** 2011. Identification of amino acids in auxiliary replicase protein p27 critical for its RNA-binding activity and the assembly of the replicase complex in Red clover necrotic mosaic virus. Virology **413:**300-309.

22. **Iki, T., M. Yoshikawa, T. Meshi, and M. Ishikawa.** 2011. Cyclophilin 40 facilitates HSP90-mediated RISC assembly in plants. EMBO J **31:**267-278.

23. **Iki, T., M. Yoshikawa, M. Nishikiori, M. C. Jaudal, E. Matsumoto-Yokoyama, I. Mitsuhara, T. Meshi, and M. Ishikawa.** 2010. In vitro assembly of plant RNA-induced silencing complexes facilitated by molecular chaperone HSP90. Mol. Cell **39:**282-291.

24. **Ishibashi, K., K. Masuda, S. Naito, T. Meshi, and M. Ishikawa.** 2007. An inhibitor of viral RNA replication is encoded by a plant resistance gene. Proc. Natl. Acad. Sci. U. S. A**. 104:**13833-13838.

25. **Ishibashi, K., S. Naito, T. Meshi, and M. Ishikawa.** 2009. An inhibitory interaction between viral and cellular proteins underlies the resistance of tomato to nonadapted tobamoviruses. Proc. Natl. Acad. Sci. U. S. A**. 106:**8778-8783.

26. **Ivanovic, T., M. A. Agosto, K. Chandran, and M. L. Nibert.** 2007. A role for molecular chaperone Hsc70 in reovirus outer capsid disassembly. J. Biol. Chem. **282:**12210-12219.

27. **Iwakawa, H., A. Mine, K. Hyodo, M. N. An, M. Kaido, K. Mise, and T. Okuno.** 2011. Template recognition mechanisms by replicase proteins differ between bipartite positive-strand genomic RNAs of a plant virus. J. Virol. **85:**497-509.

28. **Iwakawa, H. O., M. Kaido, K. Mise, and T. Okuno.** 2007. cis-Acting core RNA elements required for negative-strand RNA synthesis and cap-independent

translation are separated in the 3'-untranslated region of *Red clover necrotic mosaic virus* RNA1. Virology **369:**168-181.

29. **Iwakawa, H. O., H. Mizumoto, H. Nagano, Y. Imoto, K. Takigawa, S. Sarawaneeyaruk, M. Kaido, K. Mise, and T. Okuno.** 2008. A viral noncoding RNA generated by *cis*-element-mediated protection against 5 '-> 3 ' RNA decay represses both cap-independent and cap-dependent translation. J. Virol. **82:**10162-10174.

30. **Iwakawa, H. O., Y. Tajima, T. Taniguchi, M. Kaido, K. Mise, Y. Tomari, H. Taniguchi, and T. Okuno.** 2012. Poly(A)-binding protein facilitates translation of an uncapped/nonpolyadenylated viral RNA by binding to the 3' untranslated region. J Virol. **86**:7836-49

31. **Iwasaki, S., M. Kobayashi, M. Yoda, Y. Sakaguchi, S. Katsuma, T. Suzuki, and Y. Tomari.** 2010. Hsc70/Hsp90 chaperone machinery mediates ATP-dependent RISC loading of small RNA duplexes. Mol. Cell **39:**292-299.

32. **Jaag, H. M., and P. D. Nagy.** 2010. The combined effect of environmental and host Factors on the emergence of viral RNA recombinants. Plos Pathogens **6**:e1001156

33. **Jaag, H. M., J. Pogany, and P. D. Nagy.** 2010. A host Ca2+/Mn2+ ion pump is a factor in the emergence of viral RNA recombinants. Cell Host Microbe **7:**74-81.

34. **Kaido, M., N. Funatsu, Y. Tsuno, K. Mise, and T. Okuno.** 2011. Viral cell-to-cell movement requires formation of cortical punctate structures containing Red clover necrotic mosaic virus movement protein. Virology **413:**205-215.

35. **Kaido, M., Y. Inoue, Y. Takeda, K. Sugiyama, A. Takeda, M. Mori, A. Tamai, T. Meshi, T. Okuno, and K. Mise.** 2007. Downregulation of the

NbNACa1 gene encoding a movement-protein-interacting protein reduces cell-to-cell movement of brome mosaic virus in *Nicotiana benthamiana*. Mol. Plant-Microbe Interact. **20:**671-681.

36. **Kaido, M., Y. Tsuno, K. Mise, and T. Okuno.** 2009. Endoplasmic reticulum targeting of the *Red clover necrotic mosaic virus* movement protein is associated with the replication of viral RNA1 but not that of RNA2. Virology **395:**232-242..

37. **Kampinga, H. H., and E. A. Craig.** 2010. `The HSP70 chaperone machinery: J proteins as drivers of functional specificity. Nat. Rev. Mol. Cell Biol. **11:**579-592.

38. **Kanzaki, H., H. Saitoh, A. Ito, S. Fujisawa, S. Kamoun, S. Katou, H. Yoshioka, and R. Terauchi.** 2003. Cytosolic HSP90 and HSP70 are essential components of INF1-mediated hypersensitive response and non-host resistance to Pseudomonas cichorii in *Nicotiana benthamiana*. Mol. Plant Pathol. **4:**383-391.

39. **Kim, K. H., and S. A. Lommel.** 1994. Identification and analysis fo the sote of -1 ribosomal frameshifting in *Red clover necrotic mosaic virus*. Virology **200:**574-582.

40. **Komoda, K., S. Naito, and M. Ishikawa.** 2004. Replication of plant RNA virus genomes in a cell-free extract of evacuolated plant protoplasts. Proc. Natl. Acad. Sci. U. S. A**. 101:**1863-1867.

41. **Kusumanegara K., A. Mine, K. Hyodo, M. Kaido, K. Mise, and T. Okuno.** in press. Identification of domains in p27 auxiliary replicase proteins essential for its association with the endoplasmic reticulum membranes in *Red clover necrotic mosaic virus*. Virology.

42. **Laemmli, U. K.** 1970. Cleavage of structural proteins during assembly of head

of bacteriophage T4. Nature **227:**680-685.

43. **Leu, J. I. J., J. Pimkina, A. Frank, M. E. Murphy, and D. L. George.** 2009. A small molecule inhibitor of inducible heat shock protein 70. Mol. Cell **36:**15-27.

44. **Leu, J. I. J., J. Pimkina, P. Pandey, M. E. Murphy, and D. L. George.** 2011. HSP70 inhibition by the small-molecule 2-phenylethynesulfonamide impairs protein clearance pathways in tumor cells. Mol. Cancer Res. **9:**936-947.

45. **Li, G., J. J. Zhang, X. M. Tong, W. J. Liu, and X. Ye.** 2011. Heat shock protein 70 inhibits the activity of influenza A virus ribonucleoprotein and bocks the replication of virus in vitro and in vivo. PLoS ONE **6**.

46. **Li, P. P., N. Itoh, M. Watanabe, Y. F. Shi, P. N. Liu, H. J. Yang, and H. Kasamatsu.** 2009. Association of simian virus 40 Vp1 with 70-kilodalton heat shock proteins and viral tumor antigens. J. Virol. **83:**37-46.

47. **Li, Z. H., J. Pogany, S. Tupman, A. M. Esposito, T. G. Kinzy, and P. D. Nagy.** 2010. Translation elongation factor 1A facilitates the assembly of the tombusvirus replicase and stimulates minus-strand synthesis. PLoS Pathog. **6**: e1001175.

48. **Lommel, S. A., M. Westonfina, Z. Xiong, and G. P. Lomonossoff.** 1988. The nucleotide sequence and gene organization of *Red clover necrotic mosaic virus* RNA2. Nucleic Acids Res. **16:**8587-8602.

49. **Magliery, T. J., C. G. M. Wilson, W. L. Pan, D. Mishler, I. Ghosh, A. D. Hamilton, and L. Regan.** 2005. Detecting protein-protein interactions with a green fluorescent protein fragment reassembly trap: Scope and mechanism. J. Am. Chem. Soc. **127:**146-157.

50. **Mas, A., I. Alves-Rodrigues, A. Noueiry, P. Ahlquist, and J. Diez.** 2006. Host deadenylation-dependent mRNA decapping factors are required for a key step in

brome mosaic virus RNA replication. J. Virol. **80:**246-251.

51. **Mayer, M. P., and B. Bukau.** 2005. Hsp70 chaperones: Cellular functions and molecular mechanism. Cell. Mol. Life Sci. **62:**670-684.

52. **Mine, A., K. Hyodo, A. Takeda, M. Kaido, K. Mise, and T. Okuno.** 2010. Interactions between p27 and p88 replicase proteins of Red clover necrotic mosaic virus play an essential role in viral RNA replication and suppression of RNA silencing via the 480-kDa viral replicase complex assembly. Virology **407:**213-224.

53. **Mine, A., A. Takeda, T. Taniguchi, H. Taniguchi, M. Kaido, K. Mise, and T. Okuno.** 2010. Identification and characterization of the 480-kilodalton template-specific RNA-dependent RNA polymerase complex of *Red clover necrotic mosaic virus*. J. Virol. **84:**6070-6081.

54. **Mitsuhara, I., M. Ugaki, H. Hirochika, M. Ohshima, T. Murakami, Y. Gotoh, Y. Katayose, S. Nakamura, R. Honkura, S. Nishimiya, K. Ueno, A. Mochizuki, H. Tanimoto, H. Tsugawa, Y. Otsuki, and Y. Ohashi.** 1996. Efficient promoter cassettes for enhanced expression of foreign genes in dicotyledonous and monocotyledonous plants. Plant Cell Physiol. **37:**49-59.

55. **Miyoshi, T., A. Takeuchi, H. Siomi, and M. C. Siomi.** 2010. A direct role for Hsp90 in pre-RISC formation in Drosophila. Nat. Struct. Mol. Biol. **17:**1024-1026.

56. **Mizumoto, H., Y. Hikichi, and T. Okuno.** 2002. The 3 '-untranslated region of RNA1 as a primary determinant of temperature sensitivity of *Red clover necrotic mosaic virus* Canadian strain. Virology **293:**320-327.

57. **Mizumoto, H., H. O. Iwakawa, M. Kaido, K. Mise, and T. Okuno.** 2006. Cap-independent translation mechanism of Red clover necrotic mosaic virus RNA2 differs from that of RNA1 and is linked to RNA replication. J. Virol.

80:3781-3791.

58. **Mizumoto, H., M. Tatsuta, M. Kaido, K. Mise, and T. Okuno.** 2003. Cap-independent translational enhancement by the 3 ' untranslated region of *Red lover necrotic mosaic virus* RNA1. J. Virol. **77:**12113-12121.

59. **Momose, F., T. Naito, K. Yano, S. Sugimoto, Y. Morikawa, and K. Nagata.** 2002. Identification of Hsp90 as a stimulatory host factor involved in influenza virus RNA synthesis. J. Biol. Chem. **277:**45306-45314.

60. **Murata, S., H. Yashiroda, and K. Tanaka.** 2009. Molecular mechanisms of proteasome assembly. Nat. Rev. Mol. Cell Biol. **10:**104-115.

61. **Nagy, P. D., and J. Pogany.** 2012. The dependence of viral RNA replication on co-opted host factors. Nat. Rev. Microbiol. **10:**137-149.

62. **Nagy, P. D., R. Y. Wang, J. Pogany, A. Hafren, and K. Makinen.** 2011. Emerging picture of host chaperone and cyclophilin roles in RNA virus replication. Virology **411:**374-382.

63. **Naito, T., F. Momose, A. Kawaguchi, and K. Nagata.** 2007. Involvement of Hsp90 in assembly and nuclear import of influenza virus RNA polymerase subunits. J. Virol. **81:**1339-1349.

64. **Nishikiori, M., K. Dohi, M. Mori, T. Meshi, S. Naito, and M. Ishikawa.** 2006. Membrane-bound tomato mosaic virus replication proteins participate in RNA synthesis and are associated with host proteins in a pattern distinct from those that are not membrane bound. J. Virol. **80:**8459-8468.

65. **Noueiry, A. O., J. Diez, S. P. Falk, J. B. Chen, and P. Ahlquist.** 2003. Yeast Lsm1p-7p/Pat1p deadenylation-dependent mRNA-decapping factors are required for brome mosaic virus genomic RNA translation. Mol Cell Biol **23:**4094-4106.

66. **Okamoto, K., H. Nagano, H. Iwakawa, H. Mizumoto, A. Takeda, M. Kaido,**

K. Mise, and T. Okuno. 2008. cis-Preferential requirement of a-1 frameshift product p88 for the replication of Red clover necrotic mosaic virus RNA1. Virology **375:**205-212.

67. **Okamoto, T., Y. Nishimura, T. Ichimura, K. Suzuki, T. Miyamura, T. Suzuki, K. Moriishi, and Y. Matsuura.** 2006. Hepatitis C virus RNA replication is regulated by FKBP8 and Hsp90. EMBO J. **25:**5015-5025.

68. **Padmanabhan, M. S., S. P. Gorepoker, S. Golem, H. Shiferaw, and J. N. Culver.** 2005. Interaction of the tobacco mosaic virus replicase protein with the Aux/IAA protein PAPI/IAA26 is associated with disease development. J. Virol. **79:**2549-2558.

69. **Padmanabhan, M. S., S. R. Kramer, X. Wang, and J. N. Culver.** 2008. Tobacco mosaic virus replicase-auxin/indole acetic acid protein interactions: Reprogramming the auxin response pathway to enhance virus infection. J. Virol. **82:**2477-2485.

70. **Pathak, K. B., J. Pogany, K. Xu, K. A. White, and P. D. Nagy.** 2012. Defining the roles of *cis*-acting RNA elements in tombusvirus replicase assembly in vitro. J Virol. **86:**156-171.

71. **Pogany, J., J. Stork, Z. H. Li, and P. D. Nagy.** 2008. In vitro assembly of the Tomato bushy stunt virus replicase requires the host Heat shock protein 70. Proc. Natl. Acad. Sci. U. S. A. **105:**19956-19961.

72. **Pogany, J., K. A. White, and P. D. Nagy.** 2005. Specific binding of tombusvirus replication protein p33 to an internal replication element in the viral RNA is essential for replication. J. Virol. **79:**4859-4869.

73. **Ratcliff, F., A. M. Martin-Hernandez, and D. C. Baulcombe.** 2001. Tobacco rattle virus as a vector for analysis of gene function by silencing. Plant J. **25:**237-245.

74. **Sarawaneeyaruk, S., H. Iwakawa, H. Mizumoto, H. Murakami, M. Kaido, K. Mise, and T. Okuno.** 2009. Host-dependent roles of the viral 5 ' untranslated region (UTR) in RNA stabilization and cap-independent translational enhancement mediated by the 3 ' UTR of *Red clover necrotic mosaic virus* RNA1. Virology **391:**107-118.

75. **Sharma, M., J. Burre, and T. C. Sudhof.** 2011. CSP alpha promotes SNARE-complex assembly by chaperoning SNAP-25 during synaptic activity. Nat. Cell Biol. **13**: 30-39

76. **Sit, T. L., A. A. Vaewhongs, and S. A. Lommel.** 1998. RNA-mediated trans-activation of transcription from a viral RNA. Science **281:**829-832.

77. **Stahl, M., J. Beck, and M. Nassal.** 2007. Chaperones activate hepadnavirus reverse transcriptase by transiently exposing a C-proximal region in the terminal protein domain that contributes to epsilon RNA binding. J. Virol. **81:**13354-13364.

78. **Stahl, M., M. Retzlaff, M. Nassal, and J. R. Beck.** 2007. Chaperone activation of the hepadnaviral reverse transcriptase for template RNA binding is established by the Hsp70 and stimulated by the Hsp90 system. Nucleic Acids Res. **35:**6124-6136.

79. **Taguwa, S., T. Okamoto, T. Abe, Y. Mori, T. Suzuki, K. Moriishi, and Y. Matsuura.** 2008. Human butyrate-induced transcript 1 interacts with hepatitis C virus NS5A and regulates viral replication. J. Virol. **82:**2631-2641.

80. **Taipale, M., D. F. Jarosz, and S. Lindquist.** 2010. HSP90 at the hub of protein homeostasis: emerging mechanistic insights. Nat. Rev. Mol. Cell Biol. **11:**515-528.

81. **Tajima, Y., H. Iwakawa, M. Kaido, K. Mise, and T. Okuno.** 2011. A long-distance RNA-RNA interaction plays an important role in programmed-1

ribosomal frameshifting in the translation of p88 replicase protein of *Red clover necrotic mosaic virus*. Virology **417:**169-178.

82. **Takabatake, R., Y. Ando, S. Seo, S. Katou, S. Tsuda, Y. Ohashi, and I. Mitsuhara.** 2007. MAP kinases function downstream of HSP90 and upstream of mitochondria in TMV resistance grene N-mediated hypersensitive cell death. Plant Cell Physiol. **48:**498-510.

83. **Takeda, A., K. Sugiyama, H. Nagano, M. Mori, M. Kaido, K. Mise, S. Tsuda, and T. Okuno.** 2002. Identification of a novel RNA silencing suppressor, NSs protein of *Tomato spotted wilt virus*. FEBS Lett. **532:**75-79.

84. **Takeda, A., M. Tsukuda, H. Mizumoto, K. Okamoto, M. Kaido, K. Mise, and T. Okuno.** 2005. A plant RNA virus suppresses RNA silencing through viral RNA replication. EMBO J **24:**3147-3157.

85. **Tanaka, S., N. Ishihama, H. Yoshioka, A. Huser, R. O'Connell, G. Tsuji, S. Tsuge, and Y. Kubo.** 2009. The Colletotrichum orbiculare SSD1 mutant enhances Nicotiana benthamiana basal resistance by activating a mitogen-activated protein kinase pathway. Plant Cell **21:**2517-2526.

86. **Tatsuta, M., H. Mizumoto, M. Kaido, K. Mise, and T. Okuno.** 2005. The Red clover necrotic mosaic virus RNA2 trans-activator is also a cis-acting RNA2 replication element. J. Virol. **79:**978-986.

87. **Tatsuta, M., H. Mizumoto, M. Kaido, K. Mise, and T. Okuno.** 2005. The Red clover necrotic mosaic virus RNA2 trans-activator is also a cis-acting RNA2 replication element. J. Virol. **79:**978-986.

88. **Turner, K. A., T. L. Sit, A. S. Callaway, N. S. Allen, and S. A. Lommel.** 2004. Red clover necrotic mosaic virus replication proteins accumulate at the endoplasmic reticulum. Virology **320:**276-290.

89. **Ujino, S., S. Yamaguchi, K. Shimotohno, and H. Takaku.** 2009. Heat-shock

protein 90 is essential for stabilization of the hepatitis C virus nonstructural protein NS3. J. Biol. Chem. **284:**6841-6846.

90. **Wang, R. Y. L., and P. D. Nagy.** 2008. Tomato bushy stunt virus co-opts the RNA-binding function of a host metabolic enzyme for viral genomic RNA synthesis. Cell Host Microbe **3:**178-187.

91. **Wang, R. Y. L., J. Stork, and P. D. Nagy.** 2009. A key role for heat shock protein 70 in the localization and insertion of tombusvirus replication proteins to intracellular membranes. J. Virol. **83:**3276-3287.

92. **Weeks, S. A., W. P. Shield, C. Sahi, E. A. Craig, S. Rospert, and D. J. Miller.** 2010. A targeted analysis of cellular chaperones reveals contrasting roles for heat shock protein 70 in flock house virus RNA replication. J. Virol. **84:**330-339.

93. **Wegrzyn, R. D., and E. Deuerling.** 2005. Molecular guardians for newborn proteins: ribosome-associated chaperones and their role in protein folding. Cell. Mol. Life Sci. **62:**2727-2738.

94. **Xiong, Z., K. H. Kim, D. Giesmancookmeyer, and S. A. Lommel.** 1993. The roles of the Red clover necrotic mosaic virus capsid and cell-to-cell movement proteins in systemic infection. Virology **192:**27-32.

95. **Xiong, Z., K. H. Kim, T. L. Kendall, and S. A. Lommel.** 1993. Synthesis of the putative Red clover necrotic mosaic virus RNA polymerase by ribosomal frameshifting in vitro. Virology **193:**213-221.

96. **Xiong, Z., and S. A. Lommel.** 1989. The complete nucleotide sequence and genome organization of Red clover necrotic mosaic virus RNA1. Virology **171:**543-554.

97. **Xiong, Z. G., and S. A. Lommel.** 1991. Red clover necrotic mosaic virus infectious transcripts synthesized in vitro. Virology **182:**388-392.

FIGURE LEGENDS

Fig. 1. Knock-down of Hsp70 or Hsp90 mRNA levels via gene silencing inhibits accumulation of RCNMV RNAs in *N. benthamiana* plants. (A) The *Tobacco rattle virus* (TRV) vector harboring the partial fragment of *N. benthamiana Hsp70c-1* (TRV:Hsp70) or *Hsp90* (TRV:Hsp90) was expressed in *N. benthamiana* by *Agrobacterium* infiltration. The empty TRV vector (TRV:00) was used as a control. Pictures were taken at 10 days after agroinfiltration (dai). Note that the infiltrated plants show no morphological defects at this stage. (B and C) The newly developed leaves were inoculated with RCNMV RNA1 and RNA2 10 days after agroinfiltration. Total RNAs were extracted from the inoculated leaves 2 days after inoculation. Accumulation of RCNMV RNAs was analyzed by northern blotting. Ethidium bromide (EtBr)-stained ribosomal RNAs (rRNA) are shown below the northern blots as loading controls. Hsp70 and Hsp90 mRNA levels were assessed by RT-PCR with primers that allow the amplification of the regions of Hsp70 and Hsp90 not present in the TRV:Hsp70 and TRV:Hsp90, respectively. RT-PCR results of the ribulose 1,5-biphosphate carboxylase small subunit gene (*RbcS*) gene demonstrate equal amounts of total RNAs used for the RT and the equal efficiency of RT-reaction in the samples.

Fig. 2. Inhibitors of Hsp70 or Hsp90 impair RCNMV RNA replication in a single cell. (A and B) Tobacco BY-2 protoplasts were inoculated with *in vitro*-transcribed RNA1 and RNA2. The inoculated protoplasts were incubated for 16 h at 17 ºC in the presence of various concentrations of 2-phenylethynesulfonamide (PES), a specific inhibitor of Hsp70. Methanesulfonamide (MS) is a non-functional analogue of PES. Total RNAs were analyzed by northern blotting. EtBr-stained rRNAs as loading controls are shown below the northern blots (A). The accumulation levels of RNA1 and RNA2 from three separate experiments using PES were quantified using NIH Image and are plotted in the

graphs (B). (C and D) BY-2 protoplasts were inoculated with pUBRC1 and pUBRC2, which transcribe RNA1 and RNA2, respectively, under the control of the *cauliflower mosaic virus* (CaMV) 35S promoter. pUEGFP, which expresses GFP mRNA driven by the CaMV 35S promoter, was also inoculated as an internal control. The inoculated protoplasts were incubated for 16 h at 17 °C in the presence of various concentrations of geldanamycin (GDA), a specific inhibitor of Hsp90. Total RNAs were analyzed by northern blotting. EtBr-stained rRNAs are shown as loading controls (C). The accumulation levels of RNA1 and RNA2 from three separate experiments were quantified using NIH Image and are plotted in the graphs (D). (E and F) BY-2 protoplasts were inoculated with RCNMV virions, and incubated with GDA as described above. Total RNAs were analyzed by northern blotting. EtBr-stained rRNAs are shown as loading controls (E). The accumulation levels of RNA1 and RNA2 from three separate experiments were quantified using NIH Image and are plotted in the graphs (F).

Fig. 3. p27 interacts with Hsp70 and Hsp90 *in planta*. (A and B) Bimolecular fluorescence complementation (BiFC) analysis of the interactions of p27 with Hsp70 and Hsp90. p27 fused to the N- or C-terminal half of YFP at the C-terminus (p27-nYFP and p27-cYFP) was expressed together with Hsp70 or Hsp90 fused to the other half of YFP at the N-terminus (cYFP-Hsp70, nYFP-Hsp70, cYFP-Hsp90, and nYFP-Hsp90) in the presence of p88, RNA2, ER-mCherry, and the suppressor p19 of *Tomato bushy stunt virus,* in *N. benthamiana* leaves by *Agrobacterium* infiltration. Right panels show the merging of mCherry and YFP as yellow color. White arrowheads indicate the large fluorescent aggregates. Bars, 20 μm. (C and D) Control experiments for the BiFC analysis. YFP fragments and p27, Hsp70 or Hsp90 were separately expressed instead of their fusion protein counterparts in the presence of p88, RNA2, ER-mCherry and p19 in

N. benthamiana leaves by *Agrobacterium* infiltration. Merged images of the YFP and ER-mCherry visualized by confocal microscopy at 4 days post agroinfiltration are shown. White arrowheads indicate the large fluorescent aggregates. Bars, 20μm. (E and F) Functional analysis of YFP fragment-fused p27 in viral RNA replication. Total RNAs and proteins extracted from agroinfiltrated leaves were analyzed by northern and western blotting, respectively. EtBr-stained rRNAs as loading controls were shown below northern blots.

Fig. 4. RCNMV RNA replication affects the subcellular localization of Hsp70 and Hsp90. Green fluorescent protein (GFP)-fused Hsp70 (GFP-Hsp70) plus ER-mCherry (A), GFP-Hsp70 plus C-terminally DsRed monomer-fused p27 (p27-DRm) plus p88 plus RNA2 (B), GFP-fused-Hsp90 (GFP-Hsp90) plus ER-mCherry (C), and GFP-Hsp90 plus p27-DRm plus p88 plus RNA2 (D) were expressed in *N. benthamiana* leaves by *Agrobacterium* infiltration. Fluorescence was visualized by confocal microscopy. The merging of the green and red fluorescence is shown as yellow color. Bars, 20 μm.

Fig. 5. p27 interacts with Hsp70 and Hsp90 *in vitro*. (A) Glutathione resin-bound GST-fused Hsp70 (GST-Hsp70) or GST-Hsp90 was incubated with the purified recombinant N-terminally His and C-terminally FLAG-tagged p27 (His-p27-FLAG). After washing, pulled-down complexes were subjected to SDS-PAGE and blotted onto a membrane. Pulled down His-p27-FLAG was detected by western blotting with anti-FLAG antibody. After detection, the separated proteins on the membrane were visualized with Ponceau S staining (Ponceau S). (B and C) A capped transcript that expresses p27-FLAG (20 nM) was added to BYL. After 2 h of incubation at 17 °C, BYL expressing p27-FLAG was incubated for 30 min at 17 °C with DMSO, PES (500

μM), or MS (500 μM) in the presence of 2 mM of a non-hydrolysable analogue of ADP (ADPβS) for the analysis of p27–Hsp70 interaction (B). Alternatively, BYL expressing p27-FLAG was incubated for 30 min at 17 °C with DMSO or GDA (500 μM) in the presence of 2 mM of a non-hydrolysable analogue of ATP (ATPγS) and 3 mM of $MgCl_2$ for the analysis of p27–Hsp90 interaction (C). The BYL was then mixed with a 10 μl bed volume of anti-FLAG M2 antibody agarose, and incubated further on ice for 90 min. After washing, Hsp70 and Hsp90 co-purified with p27-FLAG were analyzed by western blotting with appropriate antibodies.

Fig. 6. PES and GDA inhibit accumulations of p27 and negative-strand RNAs in BYL. BYL was incubated for 4 h at 17 °C with *in vitro* synthesized RNA1 (7.5 nM) and RNA2 (20 nM) in the presence of various concentrations of inhibitors. Accumulations of negative-strand RNA1 and RNA2 were detected by northern blotting. Accumulations of p27 were analyzed by western blotting with anti-p27 antisera. EtBr-stained rRNAs and CBB-stained cellular proteins are shown as loading controls.

Fig. 7. Hsp70 and Hsp90 promote the assembly of the RCNMV replicase complex. (A) Depiction of the assay system using BYL to monitor the assembly of the 480-kDa replicase complex and the synthesis of negative-strand RNA2 independently of the translation and folding of p27 and p88 replicase proteins. [1] Capped transcripts expressing p27-FLAG (20 nM) or p88-T7 (20 nM) were incubated separately in BYL for 2 h at 17 °C. [2] After the addition of cycloheximide at a concentration of 100 μg/ml, BYL expressing p27-FLAG and BYL expressing p88-T7 were mixed at 2:1 ratio. [3] RNA2 (20 nM) was added together with DMSO, PES, MS, or GDA to the mixed BYL, and incubated for an additional 2 h at 17 °C. (B) Effects of PES (500 μM) and GDA (100 μM) on the accumulation of 480-kDa complexes and the negative-strand synthesis

of RNA2. Accumulation of negative-strand RNA2 was analyzed by northern blotting. EtBr-stained rRNAs are shown below the northern blots as loading controls. Accumulation of the 480-kDa replicase complexes were analyzed by western blotting with anti-p27 antisera after the separation of protein complexes by blue native polyacrylamide gel electrophoresis (BN-PAGE). Accumulation of p27-FLAG and p88-T7 was analyzed by western blotting with anti-FLAG and anti-T7 antibodies, respectively, after separation of the denatured proteins by SDS-PAGE. CBB-stained cellular proteins are shown below the western blots as loading controls. (C-F) Dose-dependent effects of PES and GDA on the accumulation of the 480-kDa replicase complex and negative-strand RNA synthesis. BYL expressing p27-FLAG and p88-T7 were prepared and mixed as described in (A). Then, the mixed BYL was incubated with RNA2 (20 nM) for 2 h at 17 ˚C in the presence of increasing amounts of PES (C and D) or GDA (D and E). Western blots with anti-FLAG antibodies in combination with BN-PAGE detected the 480-kDa replicase complexes and nonfunctional large complexes. Western blots in combination with SDS-PAGE detected p27-FLAG and p88-T7 components. CBB-stained cellular proteins are shown as loading controls. Northern blots showed accumulations of negative-strand RNA2. EtBr-stained rRNAs are shown below the northern blots as loading controls. (G) Effects of the reduced accumulation of p88 on the negative-strand RNA2 synthesis. BYL expressing p27-FLAG, BYL expressing p88-T7, and mock-treated BYL were mixed at 2:1:0, 2:0.67:0.33, 2:0.5:0.5, and 2:0.33:0.67 in the presence of MS, and BYL expressing p27-FLAG and BYL expressing p88-T7 were mixed at 2:1 in the presence of PES (from left to right). Accumulation of viral RNAs and proteins were analyzed by northern and western blotting, respectively. EtBr-stained rRNAs and CBB-stained cellular proteins are shown below the northern and western blots as loading controls, respectively.

Fig. 8. Hsp90 regulates the specific binding of p27 to the Y-shaped RNA element (YRE) of RNA2, which is critical for the assembly of the RCNMV replicase complex. (A) Effects of a mutation in YRE that inhibits the interaction between p27 and YRE on the assembly of the 480-kDa complex. BYL expressing p27-FLAG and BYL expressing p88-T7 were mixed as shown in Fig. 7A. RNA2 or its mutant, LM8, which cannot interact with p27 (27), was added to the mixed BYL and the mixture was incubated for 2 h. Accumulation of viral RNAs was analyzed by northern blotting. Accumulation of the 480-kDa complexes and its viral components was analyzed by western blotting in combination with BN-PAGE and SDS-PAGE, respectively. (B) Effects of inhibitors on the binding of p27 with YRE. Membrane-depleted BYL (BYLS20) expressing p27-FLAG was incubated for 20 min on ice with StagT-fused YRE in the presence of PES, MS or GDA (500 μM each). Heparin was added to the BYLS20 at a final concentration of 20 μg/ml and the mixture was incubated for 40 min. The BYLS20 was subjected to Strepto-tag affinity purification, followed by western blotting with anti-FLAG antibody. The affinity-purified YRE was detected with EtBr staining.

A


TRV:00
TRV:Hsp70
TRV:Hsp90

B

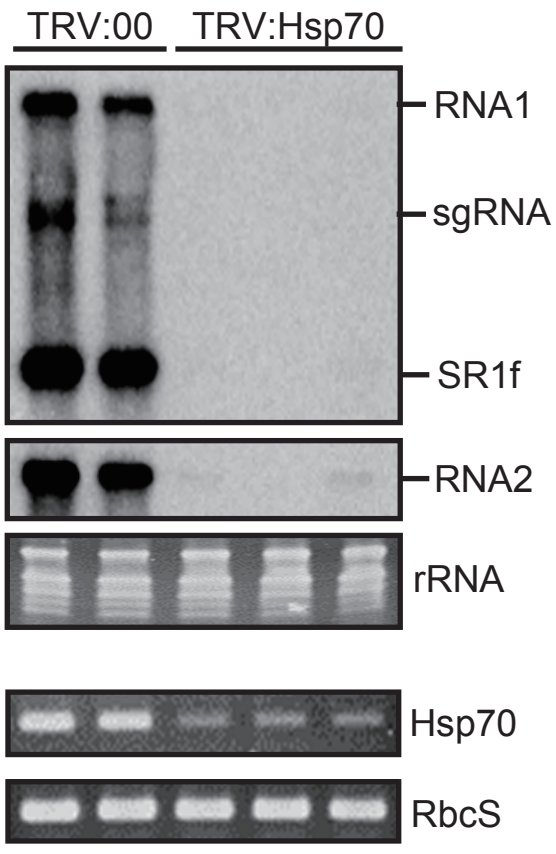
TRV:00
TRV:Hsp70
RNA1
sgRNA
SR1f
RNA2
rRNA
Hsp70
RbcS

C

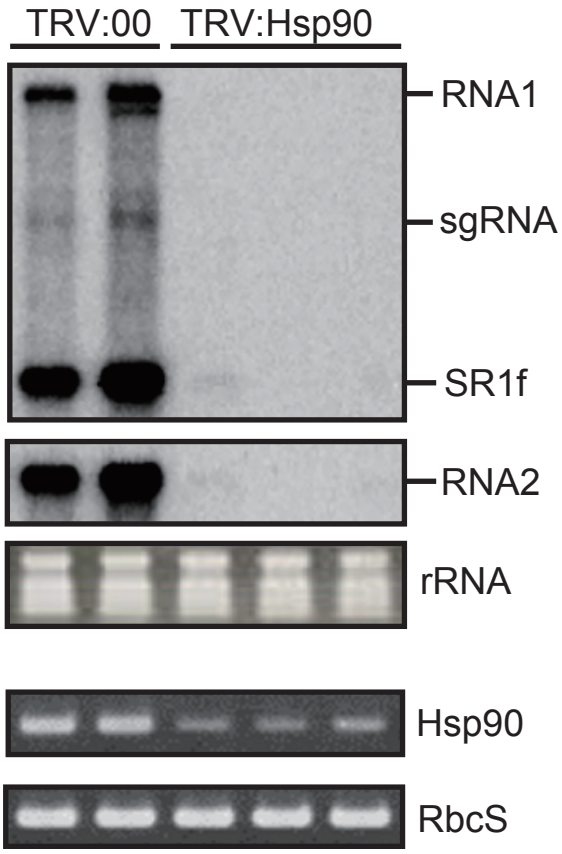
TRV:00
TRV:Hsp90
RNA1
sgRNA
SR1f
RNA2
rRNA
Hsp90
RbcS

Figure 1

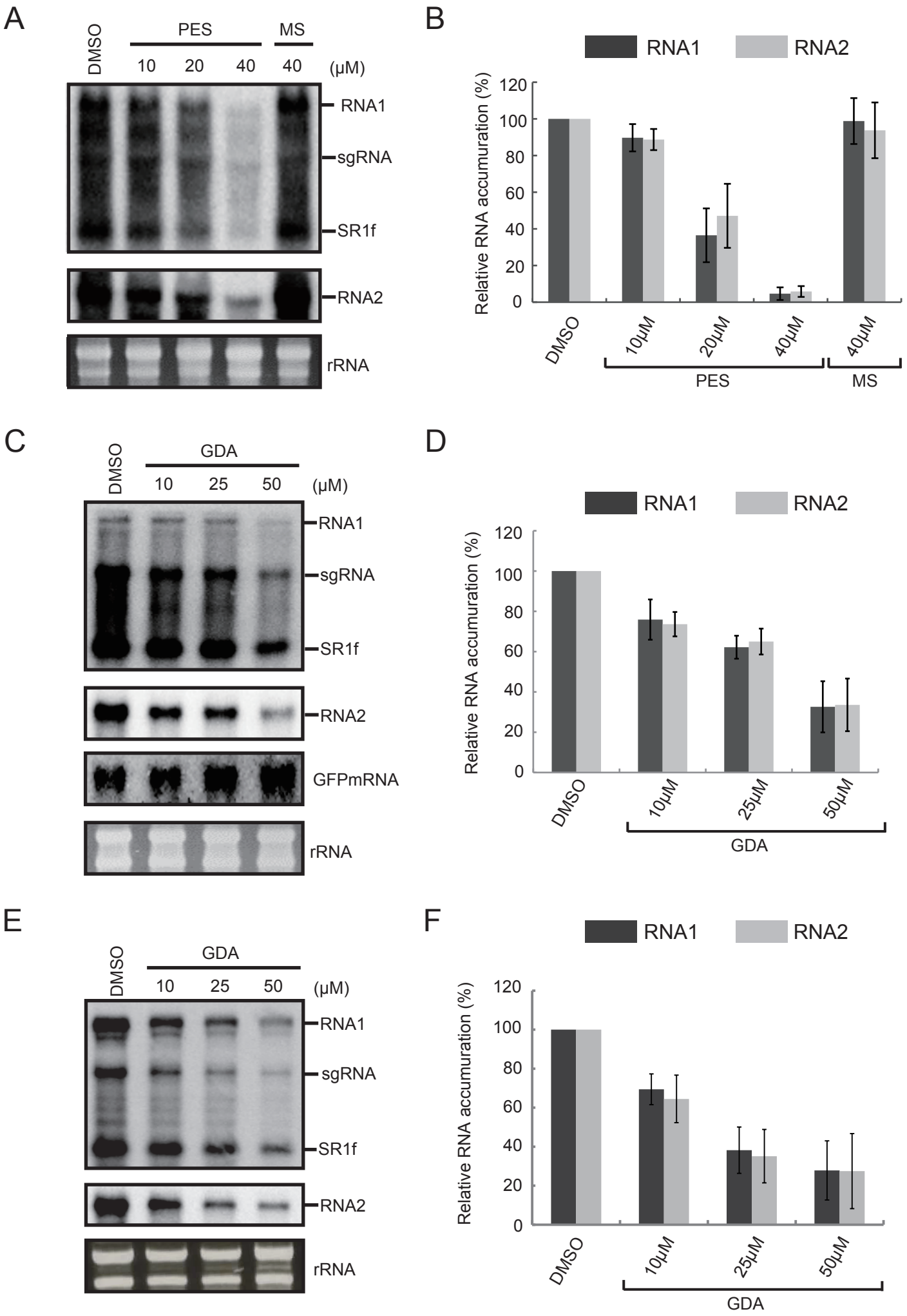
A
DMSO
PES
MS
10
20
40
40
(μM)
RNA1
sgRNA
SR1f
RNA2
rRNA
B
RNA1
RNA2
Relative RNA accumuration (%)
120
100
80
60
40
20
0
DMSO
10μM
20μM
40μM
40μM
PES
MS
C
DMSO
GDA
10
25
50
(μM)
RNA1
sgRNA
SR1f
RNA2
GFPmRNA
rRNA
D
RNA1
RNA2
Relative RNA accumuration (%)
120
100
80
60
40
20
0
DMSO
10μM
25μM
50μM
GDA
E
DMSO
GDA
10
25
50
(μM)
RNA1
sgRNA
SR1f
RNA2
rRNA
F
RNA1
RNA2
Relative RNA accumuration (%)
120
100
80
60
40
20
0
DMSO
10μM
25μM
50μM
GDA

Figure 2

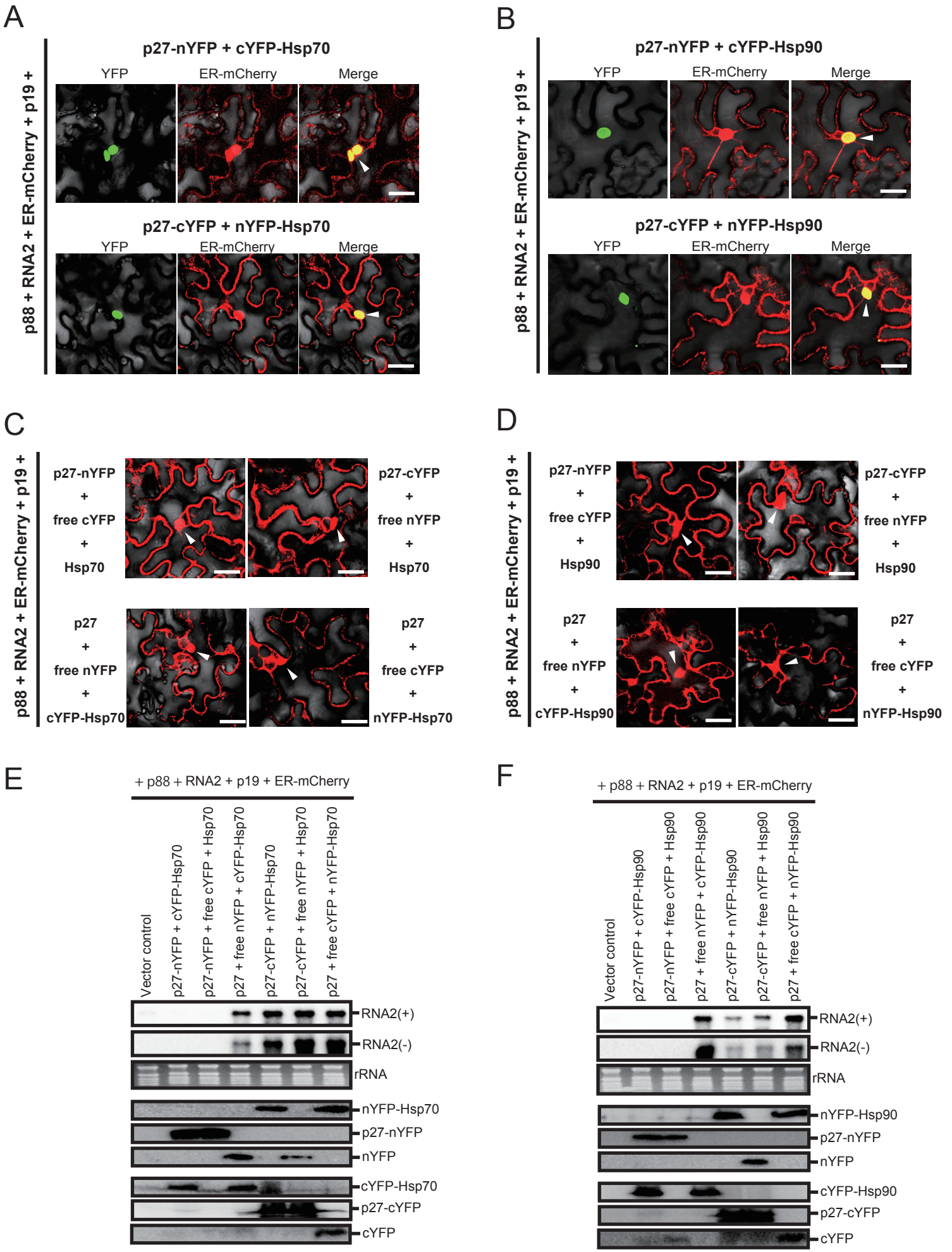
A
p88 + RNA2 + ER-mCherry + p19 +
p27-nYFP + cYFP-Hsp70
YFP
ER-mCherry
Merge
p27-cYFP + nYFP-Hsp70
B
p27-nYFP + cYFP-Hsp90
p27-cYFP + nYFP-Hsp90
C
p27-nYFP + free cYFP + Hsp70
p27-cYFP + free nYFP + Hsp70
p27 + free nYFP + cYFP-Hsp70
p27 + free cYFP + nYFP-Hsp70
D
p27-nYFP + free cYFP + Hsp90
p27-cYFP + free nYFP + Hsp90
p27 + free nYFP + cYFP-Hsp90
p27 + free cYFP + nYFP-Hsp90
E
+ p88 + RNA2 + p19 + ER-mCherry
Vector control
p27-nYFP + cYFP-Hsp70
p27-nYFP + free cYFP + Hsp70
p27 + free nYFP + cYFP-Hsp70
p27-cYFP + nYFP-Hsp70
p27-cYFP + free nYFP + Hsp70
p27 + free cYFP + nYFP-Hsp70
RNA2(+)
RNA2(-)
rRNA
nYFP-Hsp70
p27-nYFP
nYFP
cYFP-Hsp70
p27-cYFP
cYFP
F
+ p88 + RNA2 + p19 + ER-mCherry
Vector control
p27-nYFP + cYFP-Hsp90
p27-nYFP + free cYFP + Hsp90
p27 + free nYFP + cYFP-Hsp90
p27-cYFP + nYFP-Hsp90
p27-cYFP + free nYFP + Hsp90
p27 + free cYFP + nYFP-Hsp90
RNA2(+)
RNA2(-)
rRNA
nYFP-Hsp90
p27-nYFP
nYFP
cYFP-Hsp90
p27-cYFP
cYFP

Figure 3

A. GFP-Hsp70 + ER-mCherry

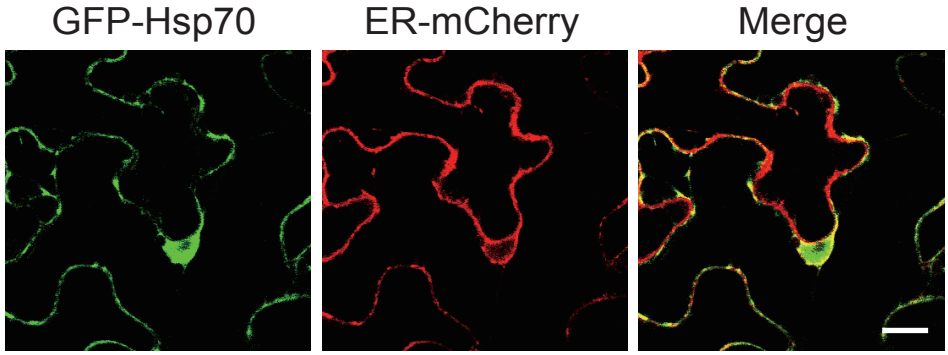

B. GFP-Hsp70 + p27-DRm + p88 + RNA2

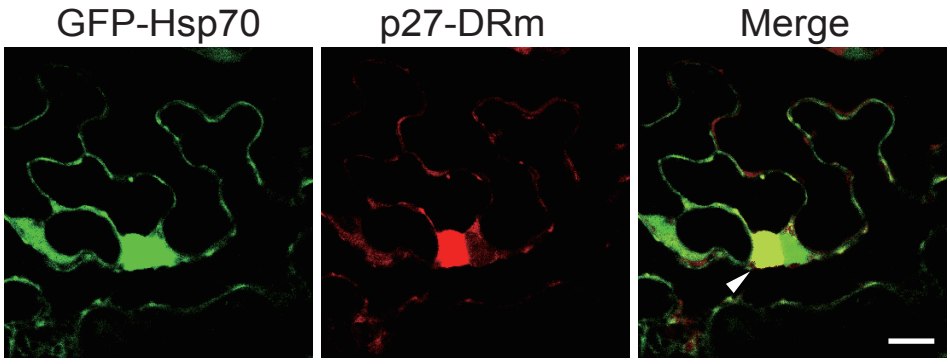

C. GFP-Hsp90 + ER-mCherry

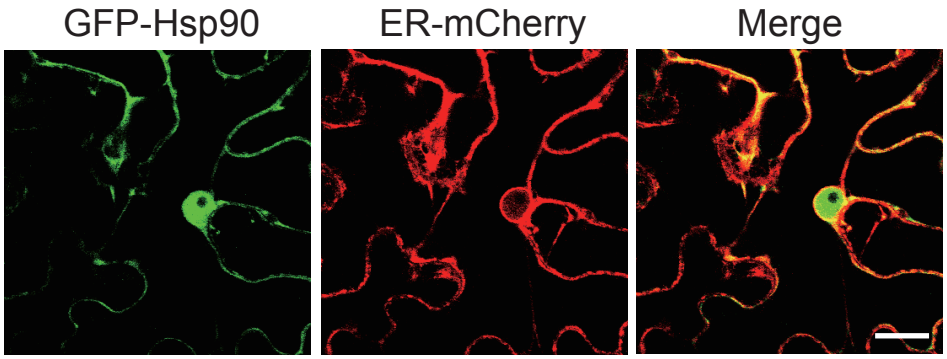

D. GFP-Hsp90 + p27-DRm + p88 + RNA2

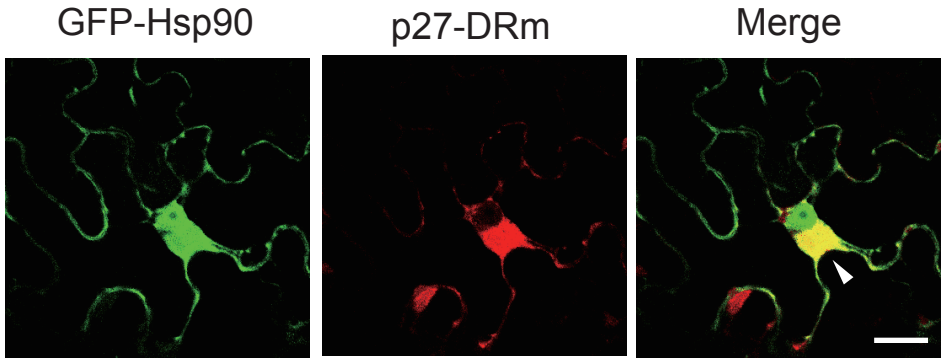

Figure 4

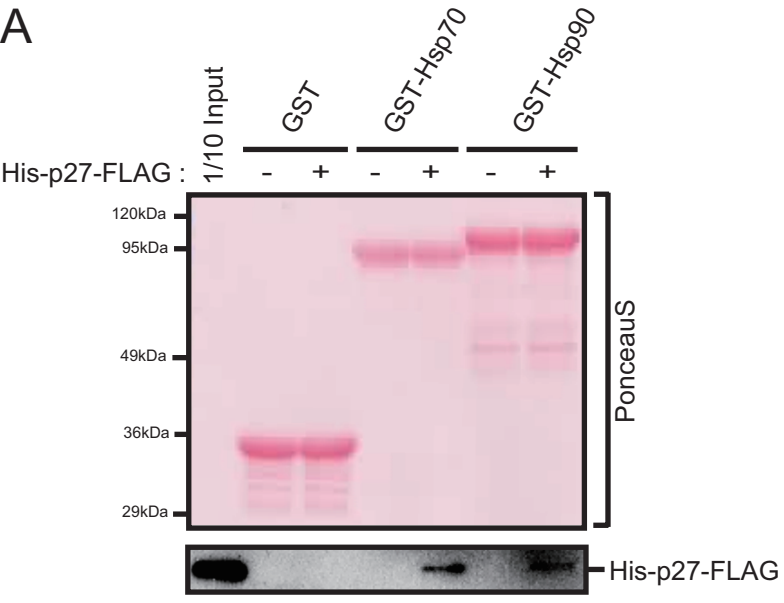
A
1/10 Input
GST
GST-Hsp70
GST-Hsp90
His-p27-FLAG :
- + - + - +
120kDa
95kDa
49kDa
36kDa
29kDa
PonceauS
His-p27-FLAG

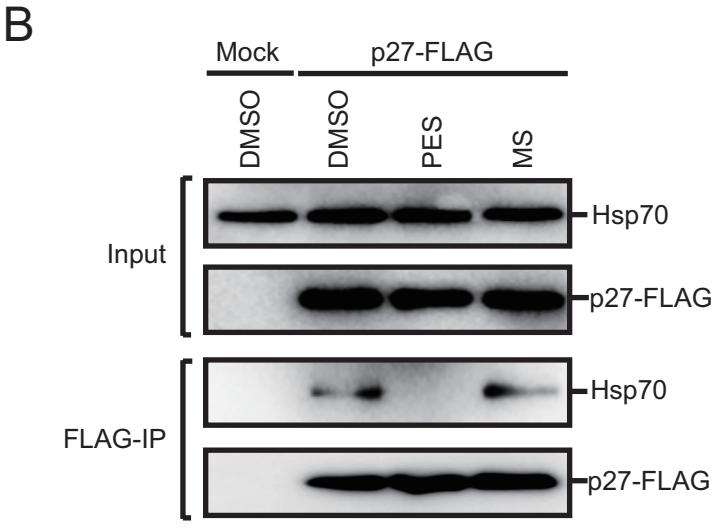
B
Mock
p27-FLAG
DMSO
DMSO
PES
MS
Input
Hsp70
p27-FLAG
FLAG-IP
Hsp70
p27-FLAG

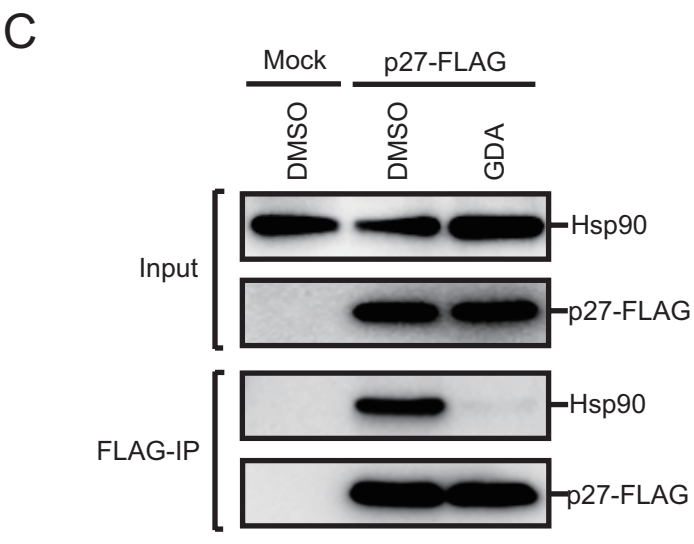
C
Mock
p27-FLAG
DMSO
DMSO
GDA
Input
Hsp90
p27-FLAG
FLAG-IP
Hsp90
p27-FLAG

Figure 5

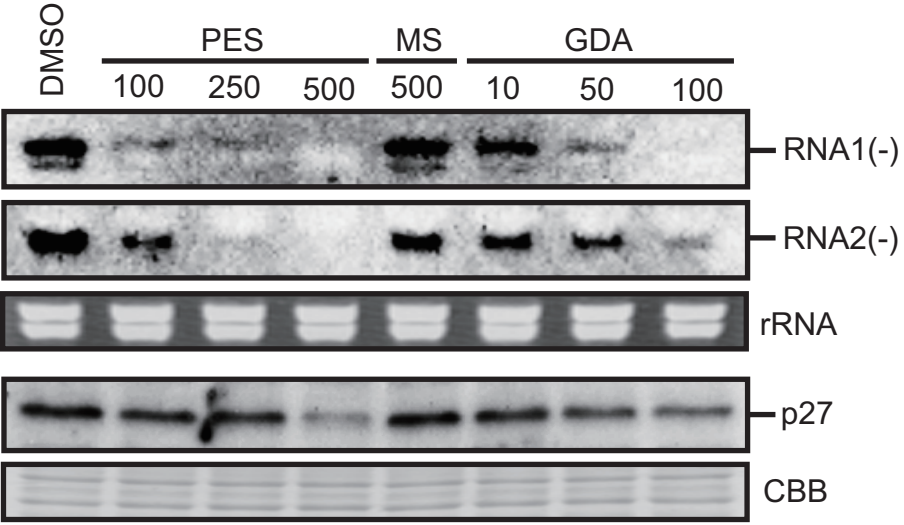

Figure 6

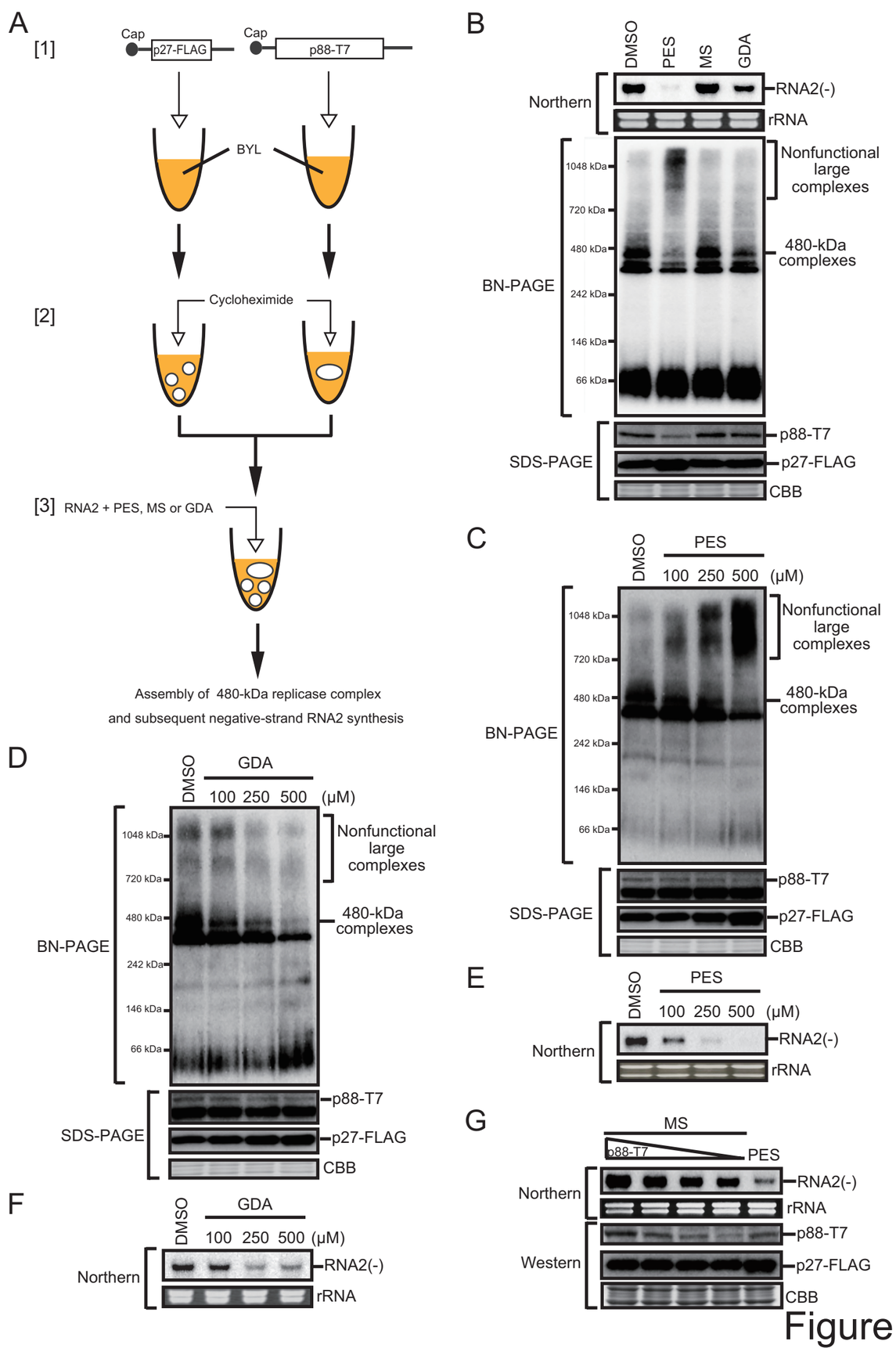
A
[1]
Cap
p27-FLAG
Cap
p88-T7
BYL
[2]
Cycloheximide
[3] RNA2 + PES, MS or GDA
Assembly of 480-kDa replicase complex
and subsequent negative-strand RNA2 synthesis
B
DMSO
PES
MS
GDA
Northern
RNA2(-)
rRNA
BN-PAGE
1048 kDa
720 kDa
480 kDa
242 kDa
146 kDa
66 kDa
Nonfunctional large complexes
480-kDa complexes
SDS-PAGE
p88-T7
p27-FLAG
CBB
C
DMSO
PES
100 250 500 (μM)
BN-PAGE
Nonfunctional large complexes
480-kDa complexes
SDS-PAGE
p88-T7
p27-FLAG
CBB
D
DMSO
GDA
100 250 500 (μM)
BN-PAGE
Nonfunctional large complexes
480-kDa complexes
SDS-PAGE
p88-T7
p27-FLAG
CBB
E
DMSO
PES
100 250 500 (μM)
Northern
RNA2(-)
rRNA
F
DMSO
GDA
100 250 500 (μM)
Northern
RNA2(-)
rRNA
G
MS
p88-T7
PES
Northern
RNA2(-)
rRNA
Western
p88-T7
p27-FLAG
CBB

Figure 7

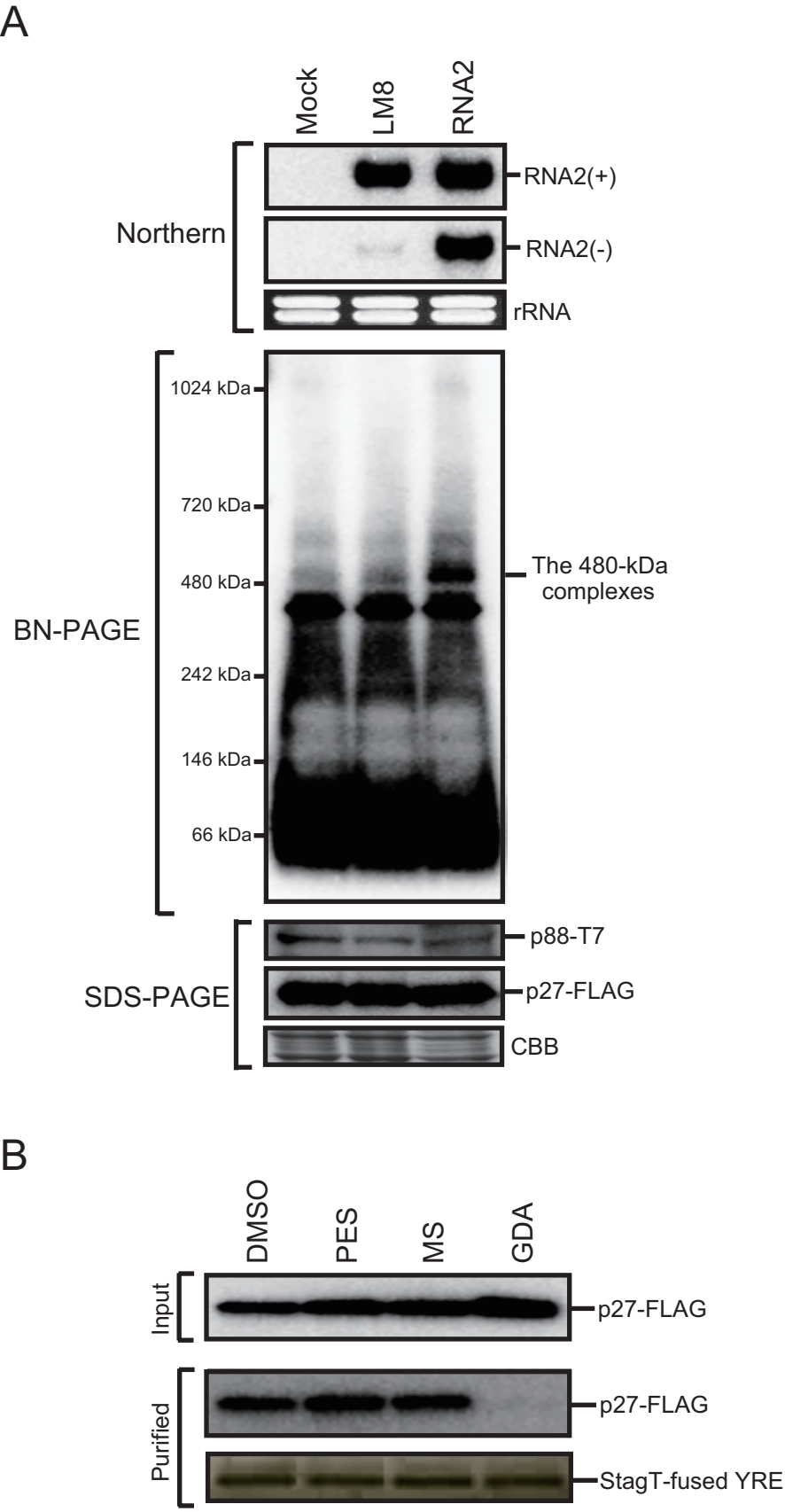
A
Mock
LM8
RNA2
Northern
RNA2(+)
RNA2(-)
rRNA
1024 kDa
720 kDa
480 kDa
242 kDa
146 kDa
66 kDa
BN-PAGE
The 480-kDa complexes
SDS-PAGE
p88-T7
p27-FLAG
CBB
B
DMSO
PES
MS
GDA
Input
p27-FLAG
Purified
p27-FLAG
StagT-fused YRE

Figure 8